NASA
Technical
Paper
2444

July 1985

Effects of Propeller Rotation Direction on Airplane Interior Noise Levels

Conrad M. Willis,
William H. Mayes,
and Edward F. Daniels

NASA

NASA Technical Paper 2444

1985

Effects of Propeller Rotation Direction on Airplane Interior Noise Levels

Conrad M. Willis,
William H. Mayes,
and Edward F. Daniels

Langley Research Center
Hampton, Virginia

National Aeronautics
and Space Administration

Scientific and Technical Information Branch

Summary

Interior noise levels have been measured in a twin-engine business airplane and in two simplified fuselage models to study the effects of propeller rotation direction. Reversal of propeller rotation direction was simulated for the models by moving the single propeller to a mirror-image position on the opposite side of the fuselage. This reversal changed the direction of the propeller tip from a downsweeping port propeller to an upsweeping starboard propeller as it moved past the juncture of the floor and fuselage sidewall. Usually, upsweeping propellers were shown to provide quieter interior noise levels than downsweeping propellers. The magnitude of the rotation direction on interior noise levels varied considerably with propeller location relative to the fuselage-floor junction and to a lesser extent with the fuselage lining and structure and with the propeller speed. Differences of up to 8 dB between upsweep and downsweep at a particular microphone location were measured for some of the test configurations.

Introduction

The development of technology for the reduction of airplane interior noise is currently receiving increased emphasis. In recent years, progress has been made both in developing and improving analytical methods for prediction of interior noise levels and in developing lightweight sidewall treatments for reducing these levels. This condition is especially true for turbofan-powered airplanes that have interior noise spectra dominated by relatively high frequency noise in the range above 500 Hz. In contrast, the interior noise levels in propeller-driven airplanes are dominated by low-frequency tones associated with the propeller blade passage harmonics and are also more difficult to control. The increased use of turboprop airplanes by commercial airlines to meet fuel-conservation goals and the proposed use of even larger and higher powered airplanes, such as the ATP (Advanced Turboprop), has provided the impetus for further development of low-frequency noise control methods.

The current technology available for predicting and reducing the interior noise for both turbofan and turboprop airplanes is reviewed by Mixson and Powell in reference 1, which also includes an extensive bibliography on the subject. In the review it is pointed out that in addition to the more traditional interior noise control methods for source noise reduction and improved fuselage sidewall treatments, noise reduction may also be obtained by the use of active noise control methods. One such method for reducing noise is propeller synchronization and phasing for multiengine propeller airplanes.

Metzger (ref. 2) presents flight measurements showing a lateral, asymmetric, interior noise field that is attributed to the effects of propeller rotation direction. It is postulated by Metzger that the lateral difference in noise levels may be due to the additional noise attenuation of the floor for the case of a propeller blade tip sweeping up past the floor-sidewall juncture on one side of the fuselage in contrast with the attenuation of the fuselage sidewall only for the blades sweeping down on the opposite side.

The purpose of this paper is to present experimental results obtained from studies using both an airplane and laboratory models to assess the effects of propeller rotation direction on interior noise. The measured interior noise contribution due to the upsweeping and downsweeping propellers on a Fairchild Merlin IVC airplane is presented. The fuselage structure is not symmetric about the vertical centerline for this airplane because the doors, windows, and structure framing are different for the port and starboard fuselage sidewalls. Since this structural asymmetry may be sufficient to affect interior noise, structurally symmetric, simplified fuselage models were fabricated and tested. This procedure enabled the evaluation of only the effects of propeller rotation direction. Additional test parameters that were not practical to vary on an airplane in flight could now also be examined. These variables included propeller tip speed, location of the propeller relative to the fuselage floor juncture, and the fuselage sidewall treatment. The relative sizes of the model structural parts are generally within the range used for general aviation aircraft but were not scaled to represent any particular fuselage design.

Symbols

C	propeller tip clearance, m
D	diameter of fuselage, m
d	axial distance from propeller plane to upstream end of cylinder interior (see fig. 12(b)), m
L	length of fuselage interior, m
M_H	helical Mach number of propeller tip
n	rotational speed of propeller, rpm
p	acoustic pressure, Pa
R_f	radius of fuselage interior, m
R_p	radius of propeller, m
r	radial coordinate, m

V_∞	free-stream velocity, knots
x	microphone axial coordinate, positive aft of propeller plane, m
β	angular location of microphone mounted on fuselage exterior with respect to line between propeller and fuselage centerlines (see fig. 5(b)), $\theta_p - \theta_m$, deg
θ	angular location of microphone or propeller, measured (counterclockwise looking forward) from top of cylinder (see fig. 12(c)), deg

Subscripts:

m	microphone
p	propeller

Abbreviations:

OASPL	overall sound pressure level
SPL	sound pressure level
Stbd	starboard side of fuselage

Airplane Experiment

Apparatus

A sketch of the Merlin IVC airplane showing the microphone locations used for this experiment is presented in figure 1. Table I summarizes the test configurations and conditions used in this investigation. The Merlin IVC, which is an executive version of the 20-passenger transport Metro III, has a 1.68-m-diameter cylindrical fuselage and two turboprop engines equipped with four-blade, 2.7-m-diameter propellers. The propellers rotate counterclockwise when viewed looking forward and have a clearance of 171 mm between the propeller tip and fuselage sidewall. With this arrangement, the port-propeller blade tips sweep up past the fuselage and the starboard propeller sweeps down.

Acoustic data were obtained from 6 interior and 10 exterior microphones during ground tests and from only the interior microphones for flight tests. Microphone locations are listed in figure 1, and a photograph of the airplane is presented in figure 2. Two Merlin IVC airplanes were used in this experiment; one was lined with fiberglass only and the other was lined with the same amount of fiberglass but also included the finish trim.

Tests

The independent effects of the port and starboard propulsion systems were determined by operating each engine separately during some of the ground run-up tests. Some of the flight data were also separated into port and starboard components by disengaging the propeller synchronizing unit and speeding up one propeller to produce a difference in blade passage frequency for the two propellers. Figure 3 shows a typical synchronizer-off spectrum of interior noise near the propeller plane. The noise for each propeller was separated into tones at frequencies corresponding to the harmonics of the respective blade passage frequency. Most of the flight data were acquired at nominal operating conditions of 3650-m altitude and 200-knot airspeed with a pressurized cabin and the engines operating at normal cruise settings. The ground run-up tests were conducted on a paved taxi strip with the airplane using approximately the same propeller rotational speed and power settings used for the flight cruise condition.

Results

Exterior noise. Noise spectra measured during airplane ground run-up tests for three locations on the fuselage exterior are presented in figure 4. Spectra for locations near the propeller disk (figs. 4(a) and 4(b)) are similar. The first-order harmonics are approximately 142 dB, both spectra have fairly regular decreasing amplitudes with increasing propeller harmonic, and both 10th harmonics have levels near 115 dB. The lowest frequency peak in the spectra occurs at about once per shaft revolution, or one-fourth the blade passage frequency of the four-blade propeller, and is more than 20 dB below the blade passage tone. Farther from the propeller plane (fig. 4(c)), the decrease in amplitude with increasing frequency is less regular and the highest amplitude tone is at the shaft frequency.

The circumferential distribution of the overall sound pressure level (OASPL) on the fuselage exterior at the propeller plane is presented in figure 5. The exterior noise level due to both propellers and the noise contribution due to each propeller at given locations on the fuselage are shown in figure 5(a). As expected, the port propeller has higher noise levels on the port fuselage surface with the highest level occurring at about the point of nearest approach ($\theta_m \approx 104°$). Similarly, the starboard propeller has higher noise levels on the starboard fuselage surface. Of particular interest is the difference in noise contributions at the top and bottom of the fuselage due to each propeller. It can be seen that the noise level from the starboard propeller is higher at the top of the fuselage ($\theta_m = 0°$), whereas the noise level from the port propeller is higher at the bottom of the fuselage ($\theta_m = 180°$). Since microphones located at the

top and bottom of the fuselage are equidistant from the port and starboard propellers, the difference in noise levels due to each propeller is believed to result from the circumferential asymmetry between the noise fields in the propeller plane ahead of and behind the blade. This acoustic asymmetry is considered essential to the existence of a direction-of-rotation effect on interior noise levels.

Figure 5(b) uses a propeller-oriented coordinate system and compares the individual patterns of noise levels due to the port and starboard propellers at corresponding β locations. Note that the angle β is measured from the reference location on the fuselage surface nearest the propeller disk. Thus, data acquired from microphones near the top of the fuselage during port engine operation are compared with starboard engine data from microphones near the bottom of the fuselage. It can be seen that overall noise levels due to the port and starboard propellers are approximately equal at corresponding β locations. Therefore, the total noise impinging on the fuselage surface from the two sources (propeller) is equal. Thus, any observed rotational effects on interior noise levels are due to the combination of the asymmetric noise field and local differences in transmission loss through the fuselage structure. The acoustic asymmetry can be seen in figure 5(b) by comparing differences in noise decay about $\beta = 0°$.

Figure 6 presents the variation in exterior OASPL with distance from the propeller tip. The noise levels on the fuselage decayed 7 dB in a distance less than 2 m aft from the propeller plane and decreased at a lower rate for additional distance. Therefore, measurement or prediction of the exterior levels for a fairly small area centered about the propeller plane should be sufficient to determine interior levels for configurations similar to the present one. The radial distribution is shown for comparison and to give some indication of the effect of tip clearance.

Interior OASPL. Figure 7(a) presents interior OASPL for both flight and ground tests with the untrimmed airplane. Higher noise levels from the starboard, or downsweeping, propeller were observed for both test conditions. The starboard propeller produced higher interior levels near the adjacent sidewall (fig. 7(b)) and also had a smaller decrease with distance across the width of the cabin. Flight data were not available for all microphone locations used for the ground tests.

A spectrum of interior noise near the propeller plane for a ground run is compared with flight levels of the blade passage tones in figure 8. The flight tones are approximately 3 dB lower than the ground data at the first harmonic, and the difference increases with harmonic order. Ground data exhibit a smoother decrease in tone amplitude with increasing harmonic order than that for the flight data. The levels of the interior tones are about 40 dB lower than the corresponding tones from the exterior spectra shown in figures 4(a) and 4(b).

Noise due to the port and starboard propellers is compared in figure 9 for the trimmed and untrimmed airplanes. The addition of trim lowered the level of the OASPL (denoted by solid symbols) and most harmonics several decibels but made little change in the difference between port and starboard noise levels. The second harmonic of the starboard propeller was higher in amplitude than any of the tones from the port propeller for both trimmed and untrimmed conditions.

Figure 10 presents averaged interior spectra for ground tests of port and starboard propellers. A one-third-octave format was used to simplify averaging of the data. The ground test data also show the same trend of more noise from the downsweeping starboard propeller that was noted for the flight data of figure 9.

Model Tests

Apparatus

Two simplified fuselage models typical of modern airplane construction were fabricated in order to study some configurations different from the airplane and to examine some test parameters over greater ranges than were practical with an airplane in flight. The models were designed to provide data for configurations having structural symmetry between the port and starboard sides. The simplified models consisted of the cylindrical fuselage and propeller only, that is, without nose, wings, or tail. The three-blade propeller had a diameter of 0.762 m and was operated at tip clearances with the fuselage of 76 and 114 mm. The propeller blade used was a model of one designed for a de Havilland Twin Otter airplane. The propeller rotated in a clockwise direction, opposite to the rotation direction of the Merlin airplane propeller.

A photograph of model 2 mounted in the quiet flow facility in the Langley Aircraft Noise Reduction Laboratory is presented in figure 11. A 1.219-m-diameter free jet issues from the floor to simulate the forward velocity of the model. A schematic plan view of the anechoic test facility is presented in figure 12(a). The propeller was inside the jet potential core, but less than half of the model fuselage was covered by the jet flow. Figure 12(b) presents a sketch of the test apparatus. The sizes of the airplane and two model fuselages are listed for comparison in the table at the top of the figure. Angular locations of the

propeller and microphone were defined by an angle θ measured from the top of the fuselage, counterclockwise looking forward, as shown in figure 12(c). The fuselage could be rotated about its longitudinal axis to locate the propeller at any desired angular location above or below the fuselage floor.

Details of the fuselage construction and microphone locations for model 1 are presented in figure 12(d). The semicircular fixture on which the microphones were mounted was attached to the axle of the model. The microphones were positioned at the desired longitudinal location by sliding the axle through the bushings (fig. 12(b)) at each end of the fuselage. The axle and mounting fixture could also be rotated up to $\pm 30^\circ$ from the position shown in the sketch (fig. 12(d)) to adjust the angular position of the microphones. The skin thickness of model 1 was 1.63 mm. The end plates that closed the cylinder were much thicker, 13 mm, so that nearly all sound transmitted to the interior would come through the sidewall. Three sidewall lining configurations were tested: a bare sidewall, a sidewall lined with a 6-mm-thick layer of acoustic foam, and a sidewall lined with lead-vinyl damping tape having a surface density of 2.44 kg/m^2. For all tests, the space below the floor was lined with two layers of material, as indicated in the sketch, and the upper side of the floor was bare.

Fabrication details for model 2 are shown in figure 12(e). Model 2 had twice the diameter of model 1, and more effort was made to simulate the structural details and to select material that might be suitable for use in an airplane fuselage. The skin was thinner than that of model 1 and was stiffened by both ring frames and stringers. A floor support web provided additional stiffness. Most of the construction was riveted. The rivet pattern for the skin-stiffener attachment can be seen in the model photograph (fig. 11). The finish trim was a 0.81-mm-thick sheet of epoxy fiberglass that was flexible enough to bend easily to the desired radius.

Only one lining configuration was tested; three layers of fiberglass were trimmed to lie between the ring frames and a fourth layer covered the inner legs of the frames. The fiberglass material had a surface density of 0.27 kg/m^2 and a nominal thickness of 13 mm with 0.05-mm-thick vinyl film on one side. The skin was lined around the complete interior circumference but the floor was left bare.

Tests

One obvious effect of reversing the propeller rotation direction is the reversal in direction of sweep of the asymmetric acoustic-aerodynamic pressure field surrounding the propeller blade that sweeps upward or downward across the fuselage with each blade passage. For a fuselage without wings, such as the models for the present test, this reversal of sweep direction of the applied exterior noise load is believed to be responsible for all changes in interior noise level. Therefore, reversal of the propeller rotation direction was simulated, as indicated schematically in figure 13, by rotating the fuselage about its longitudinal axis, thus repositioning the propeller from the port to starboard side of the fuselage with an accompanying reversal of the sweep direction. Note that the microphones were not allowed to rotate with the fuselage, and therefore they remained the same distance from the propeller after reversal.

Results

Directional effect requirements. If the structure-borne noise is neglected, the two necessary and sufficient conditions for a change in average interior noise levels due to a change in direction of propeller rotation are (1) structural asymmetry, that is, a floor that produces a circumferential variation in local transmission loss for the fuselage wall, and (2) acoustic asymmetry, that is, the difference between the noise fields in front of and behind the propeller blade. The presence of both conditions is demonstrated by the data presented in figures 14 and 15. Interior noise levels (fig. 14) were lower for most measurement locations when the propeller was located at the bottom of the fuselage than at the top, presumably because exterior noise from below the fuselage is attenuated by both fuselage sidewall and floor before reaching the cabin. The pressure time history of propeller noise presented in figure 15 exhibits a decay time between maximum and minimum pressure that is about seven times as long as the rising portion of the pulse. The propeller was not calibrated to relate the blade position to the pressure pulse, but it is believed that one side of the pulse represents the effect of an approaching blade and the other side represents a blade retreating from the microphone. This asymmetry in the pulse shape would be expected to result in an asymmetrical distribution of acoustic energy over the fuselage, and the distribution for opposite directions of rotation would be mirror images of each other.

Interior OASPL. The average interior OASPL for model 1 due to a clockwise-rotating port propeller is compared with the levels generated by simulated reversed rotation in figure 16. Three fuselage lining conditions (acoustic foam, unlined bare sidewall, and damping tape) were tested over a range of propeller speeds. A majority of the conditions examined did not exhibit a significant difference in interior OASPL

because of the reversed direction of propeller rotation; however, all three fuselage configurations tested were affected at some combinations of propeller location and propeller speed. The largest effect observed for reversed rotation during the model 1 tests was about 7 dB for the foam lining at a propeller location of $\theta_p = 105°$ and a propeller speed of 7000 rpm corresponding to a tip Mach number of about 0.6. With the damping-tape lining, reversed rotation had the most effect at 5000 rpm and $\theta_p = 150°$.

Spectra for model tests. Samples of exterior and interior spectra are presented in figure 17. Levels of the blade passage harmonics for the exterior spectrum shown are about 30 dB lower than the exterior spectrum shown for the airplane in figure 4. However, the general shape of both exterior and interior spectra are similar to those previously presented for the airplane. Again, the model interior-spectrum peaks roll off in a more irregular fashion than was observed for the exterior. Note that the fifth harmonic has disappeared in the background level of the interior spectrum.

Averaged one-third-octave spectra for clockwise and reversed rotation with model 1 at 7000 rpm are compared in figure 18. Reversed rotation produced a small reduction in noise level at the higher harmonics. Spectra from about 40 locations were averaged for the comparison of clockwise and reversed rotation presented in figure 19 for model 2. For this set of test conditions, $n = 4000$ rpm and $\theta = 135°$, rotation direction appears to have no significant effect on interior noise levels.

Comparisons. The change in average interior noise level (ΔOASPL) due to reversing the rotation direction of a downsweeping propeller for various fuselage configurations is presented in figure 20. Propeller operating conditions are identified by the helical-tip Mach number M_H, rather than by the rotational speed used in previous figures, because data for propellers of different diameters (0.8 and 2.7 m) are being compared. In figure 20(a), data for the fiberglass-lined airplane without finish trim show about the same effect of propeller reversal (ΔOASPL) as the models, except for model 1 at a Mach number M_H of 0.58. The comparison of lining conditions shown in figure 20(b) indicates that downsweeping propellers are somewhat more noisy at a majority of the propeller locations tested for model 1. However, the advantage of upsweep appears to be less for the heavy damping-tape lining than for the light foam lining.

Concluding Remarks

Tests conducted on a twin-engine business airplane and on two simple fuselage models have shown that interior noise levels can be influenced by the rotation direction of the propellers. The interior noise level was measured with rotating propeller blades sweeping both upward and downward past the fuselage. The noise was generally quieter with upsweeping blades by about 6 dB for the airplane and about 8 dB for the models. These noise differences due to upsweeping and downsweeping blades are attributed to the circumferential asymmetry of the noise field from opposite-rotating propellers combined with local differences in noise transmission loss of the fuselage structure. The model studies showed greater differences in interior noise due to direction effect with changes in propeller location relative to the fuselage-floor junction than due to differences in propeller speed or fuselage lining and trim details.

NASA Langley Research Center
Hampton, VA 23665
April 1, 1985

References

1. Mixson, John S.; and Powell, Clemans A.: Review of Recent Research on Interior Noise of Propeller Aircraft. AIAA-84-2349, Oct. 1984.
2. Metzger, Frederick B.: Strategies for Aircraft Interior Noise Reduction in Existing and Future Propeller Aircraft. SAE Tech. Paper Series 810560, Apr. 1981.

TABLE I. TEST CONFIGURATIONS AND CONDITIONS

Configuration	Cabin lining	Propeller location, θ_p, deg	n, rpm		V_∞, knots	Altitude, m
			Port	Stbd		
Merlin IVC airplane	Fiberglass	104	1570	1570	200	5350
	↓	↓	1560	1610	↓	3650
			1610	1560		3650
			1560	1560		3650
			1560	0	0	0
			0	1560	0	0
	Fiberglass + trim		1540	1600	210	3650
			1600	1540	210	3650
	↓		1600	1570	0	0
			1600	0	0	0
		↓	0	1600	0	0
Model 1	Bare	0 to 360	4000		58	0
	Bare	↓	5000		↓	↓
	Bare		7000			
	Fiberglass		7000			
	Fiberglass		↓			
	Fiberglass					
	Damping tape					
	Damping tape	↓	↓		↓	↓
Model 2	Fiberglass + trim	0 to 360	3000		46	0
		0 to 360	4000		46	0
		0 to 360	5000		46	0

Six interior microphones

No.	x, m	θ_m, deg	r, m
1	-1.50	-43	0.63
2	.43	-43	.63
3	.25	43	.63
4	2.08	43	.63
5	2.69	-43	.63
6	6.40	-43	.63

Ten exterior microphones

No.	x, m	θ_m, deg	r, m
7	0.25	0	0.84
8	.25	-45	.84
9	.25	-104	.84
10	.25	180	.84
11	.25	104	.84
12	.25	45	.84
13	1.60	-104	.84
14	4.93	-104	.84
15	0	-115	5.0
16	0	-104	6.4

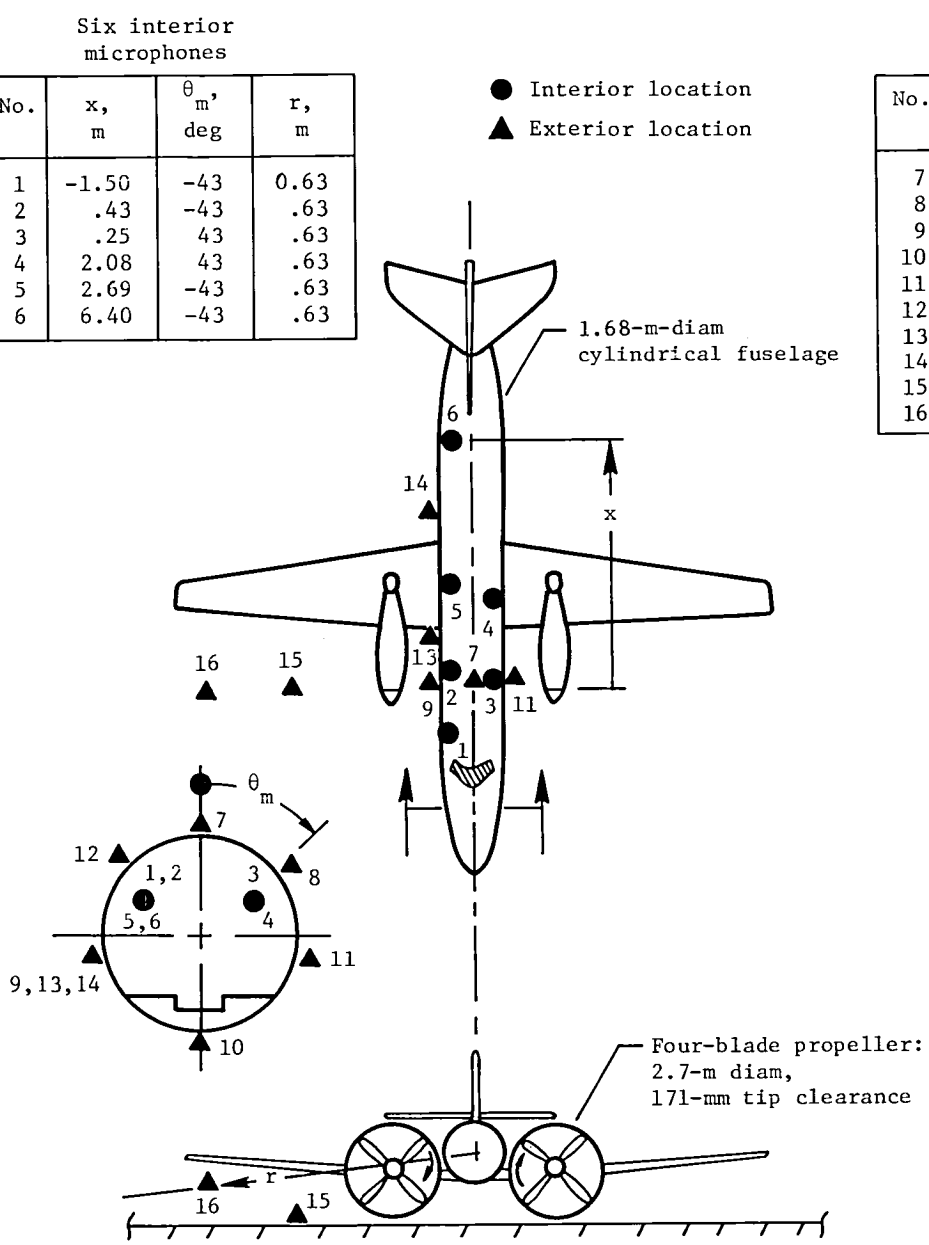

Figure 1. Sketch of Merlin IVC airplane showing microphone locations used for test of trimmed configuration.

L-83-5501

Figure 2. Photograph of Merlin IVC airplane.

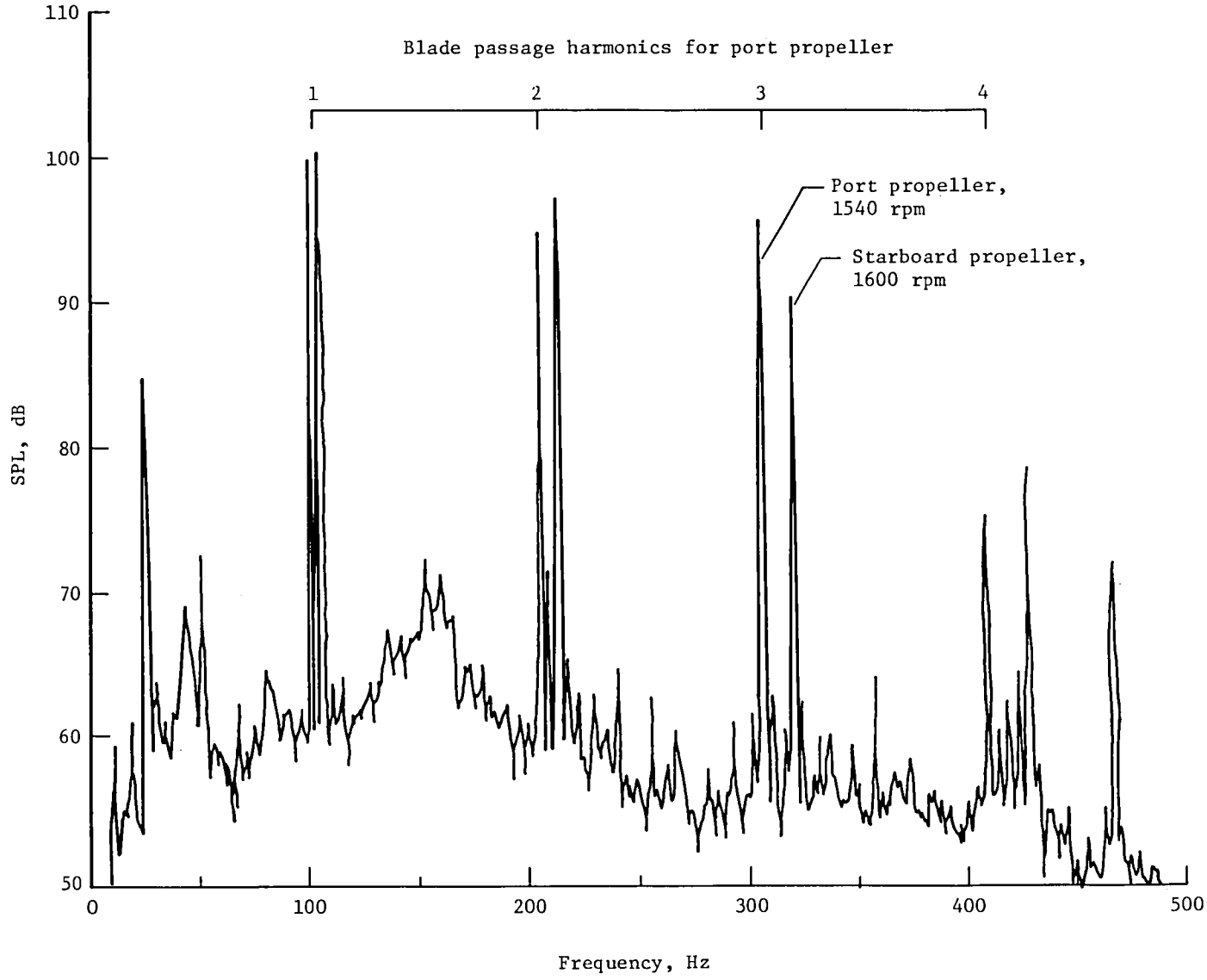

Figure 3. Spectrum illustrating extraction of data for individual propeller by use of unsynchronized propellers. Interior microphone 3 near propeller plane; 210-knot airspeed.

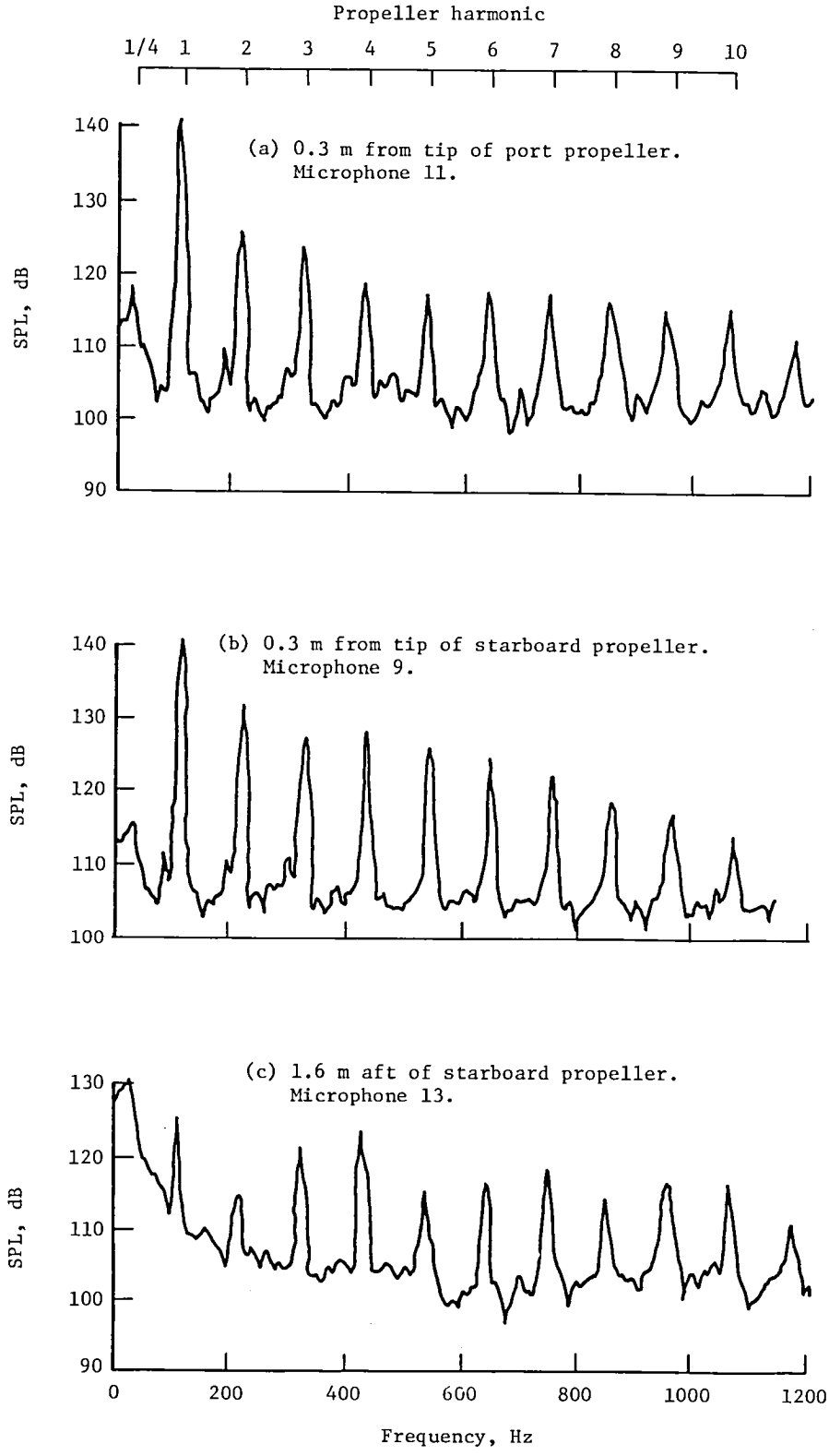

Figure 4. Typical exterior spectra for three locations on fuselage.

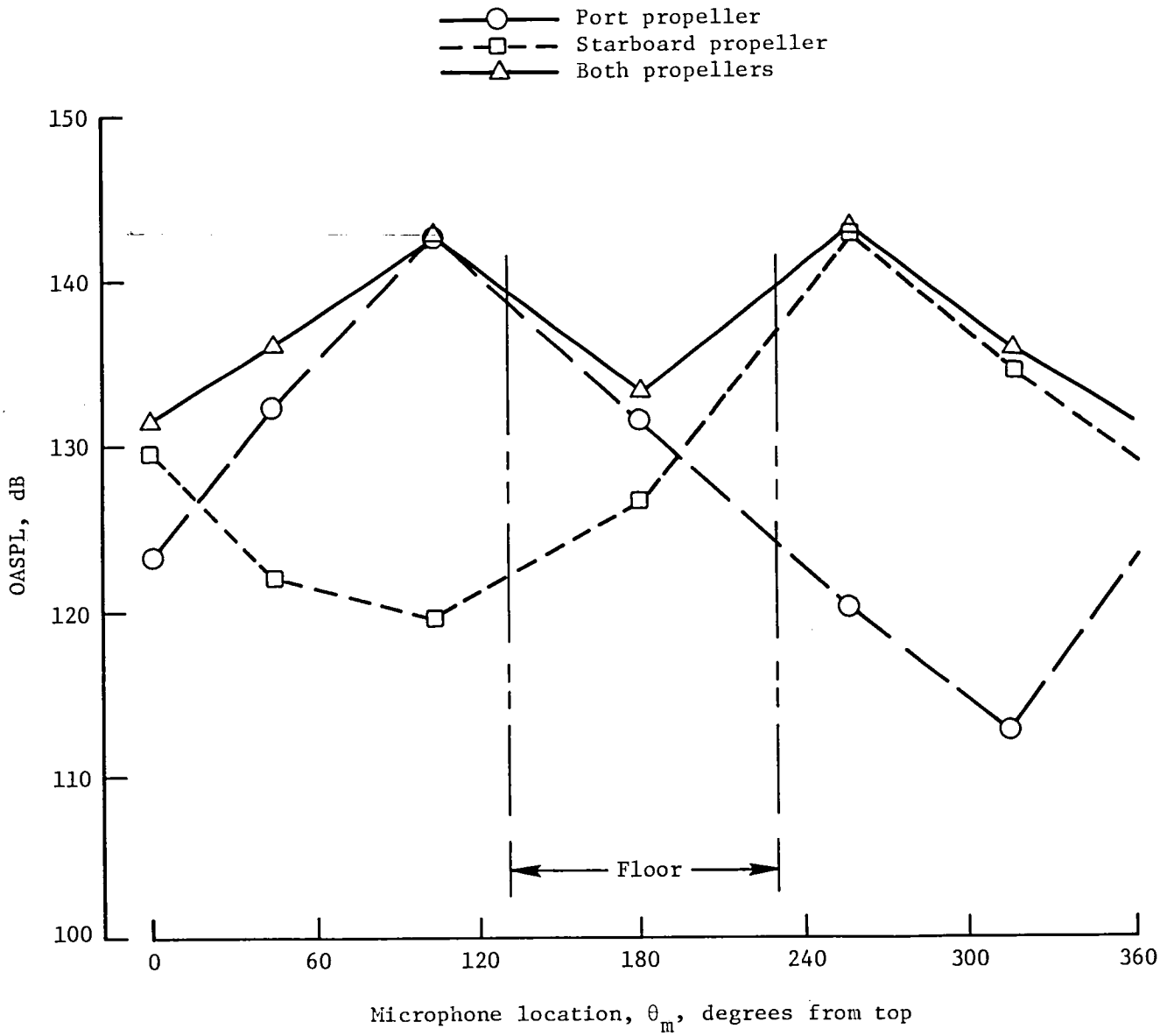

(a) Comparison of OASPL for one and two propeller operations.

Figure 5. Circumferential distribution of noise on fuselage exterior at propeller plane. Ground test.

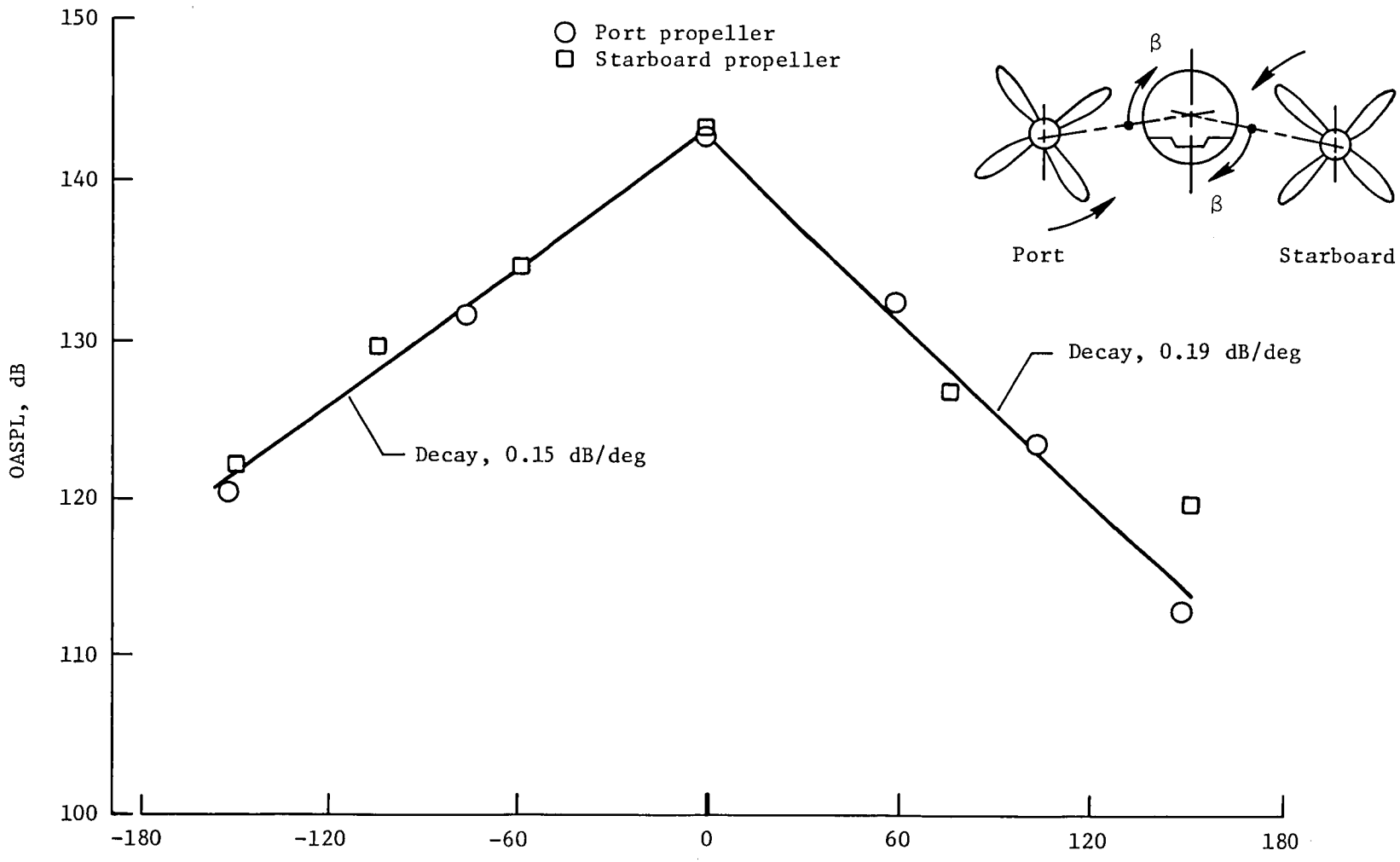

(b) Comparison of noise received from port and starboard propellers.

Figure 5. Concluded.

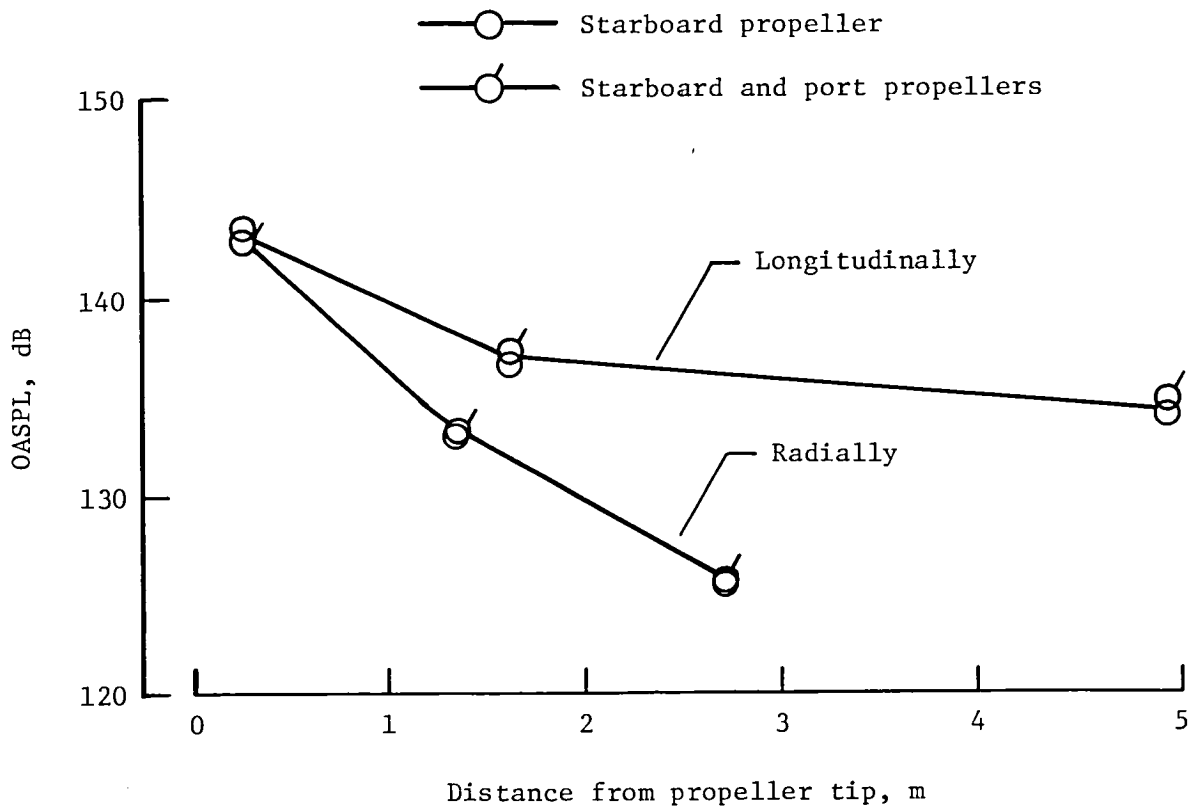

Figure 6. Variation of exterior noise with distance from propeller tip for two directions. Microphones 9, 13, 14, 15, and 16.

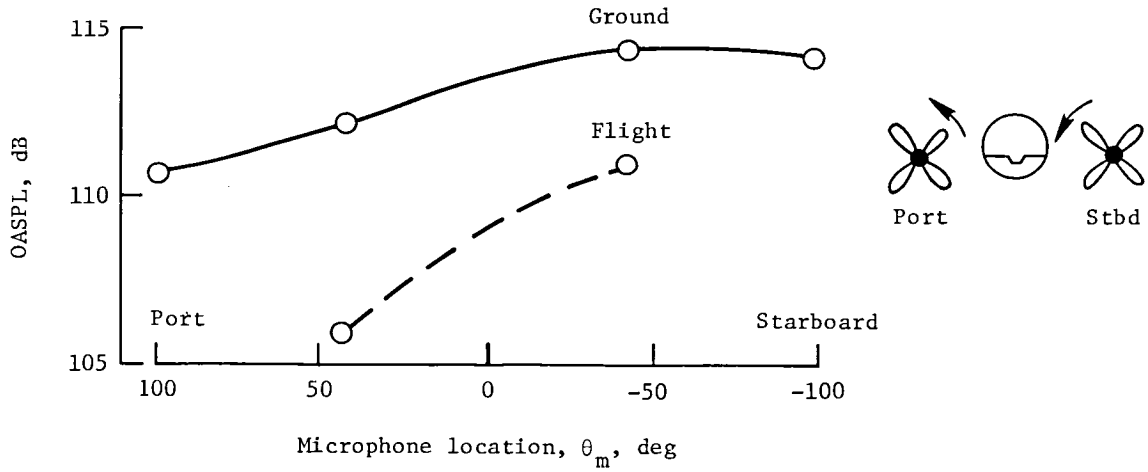

(a) Noise levels for both engines operating.

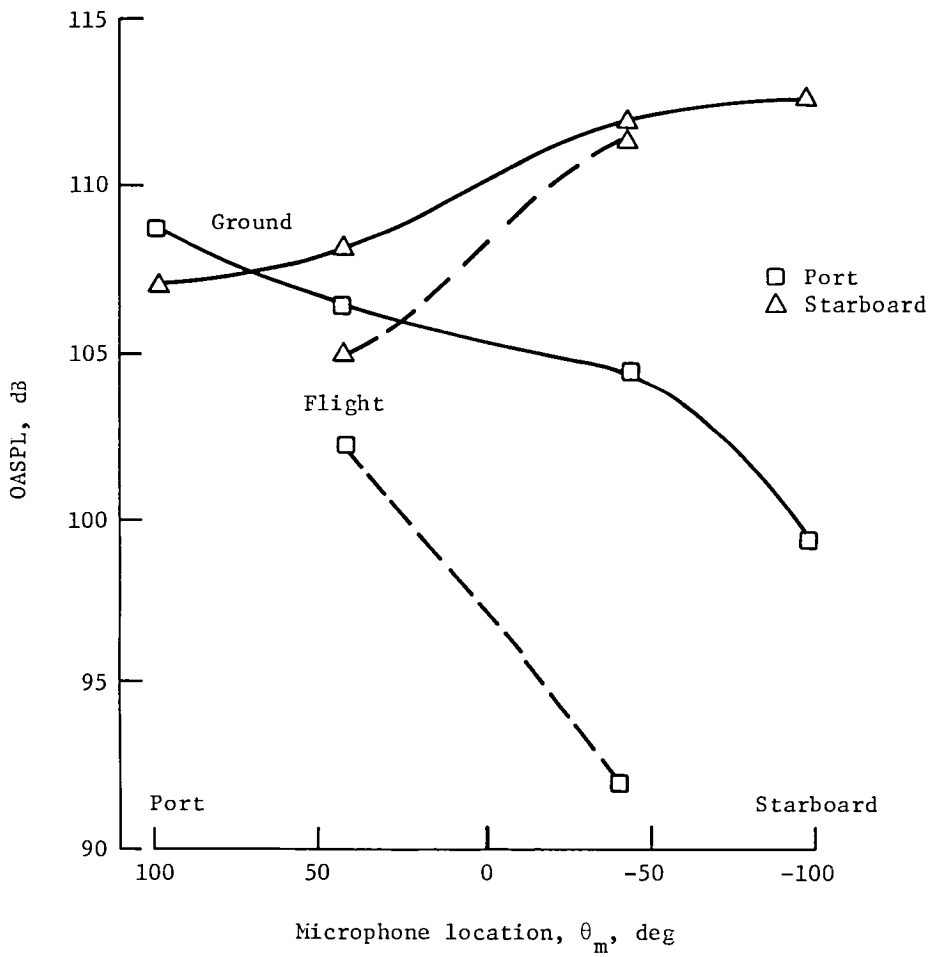

(b) Noise levels for one engine operating.

Figure 7. Circumferential variation of interior OASPL in untrimmed two-engine airplane. 0.3 m aft of propeller plane.

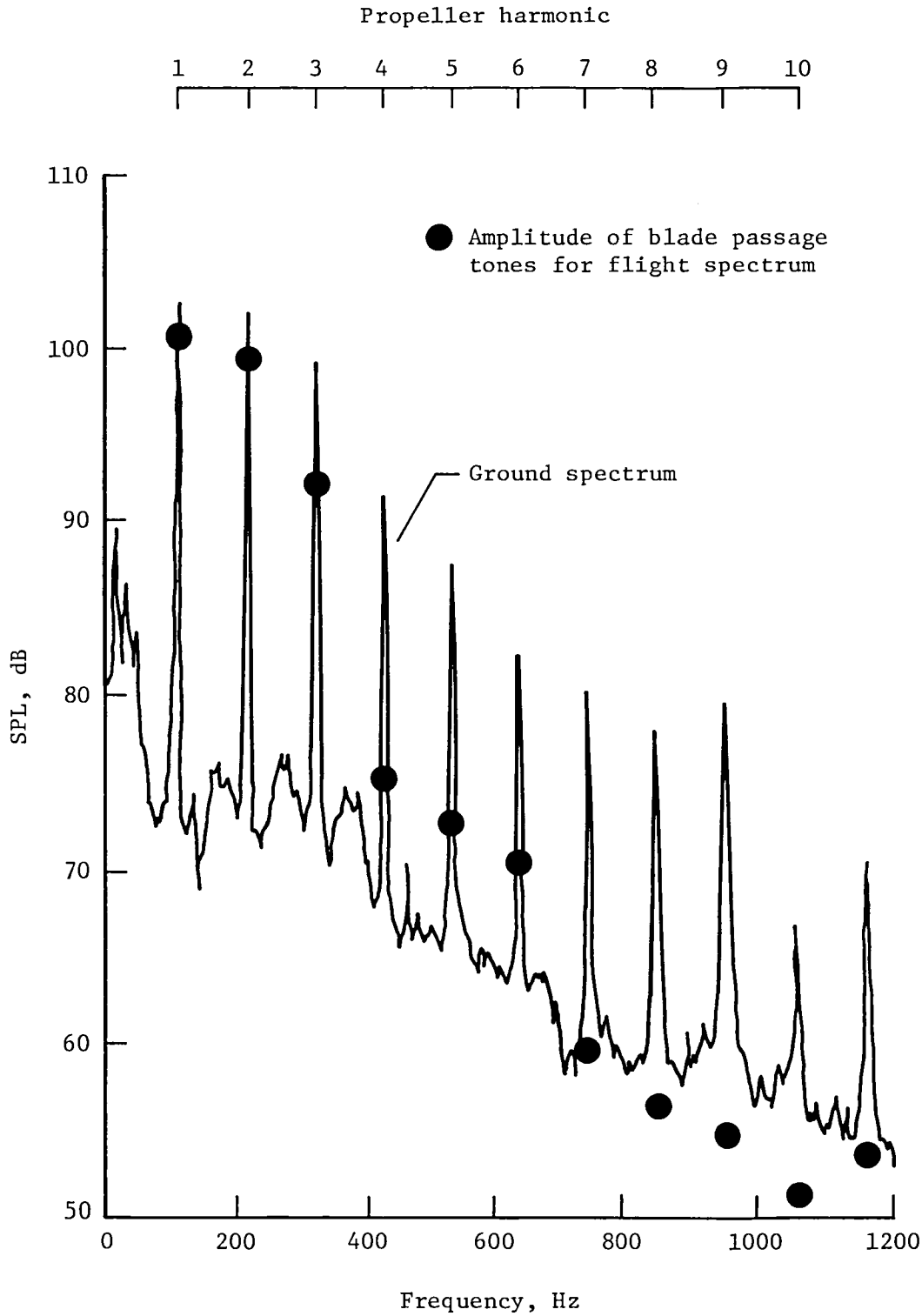

Figure 8. Comparison of interior levels for blade passage tones from ground and flight data. About 0.4 m aft of propeller plane; microphone 2.

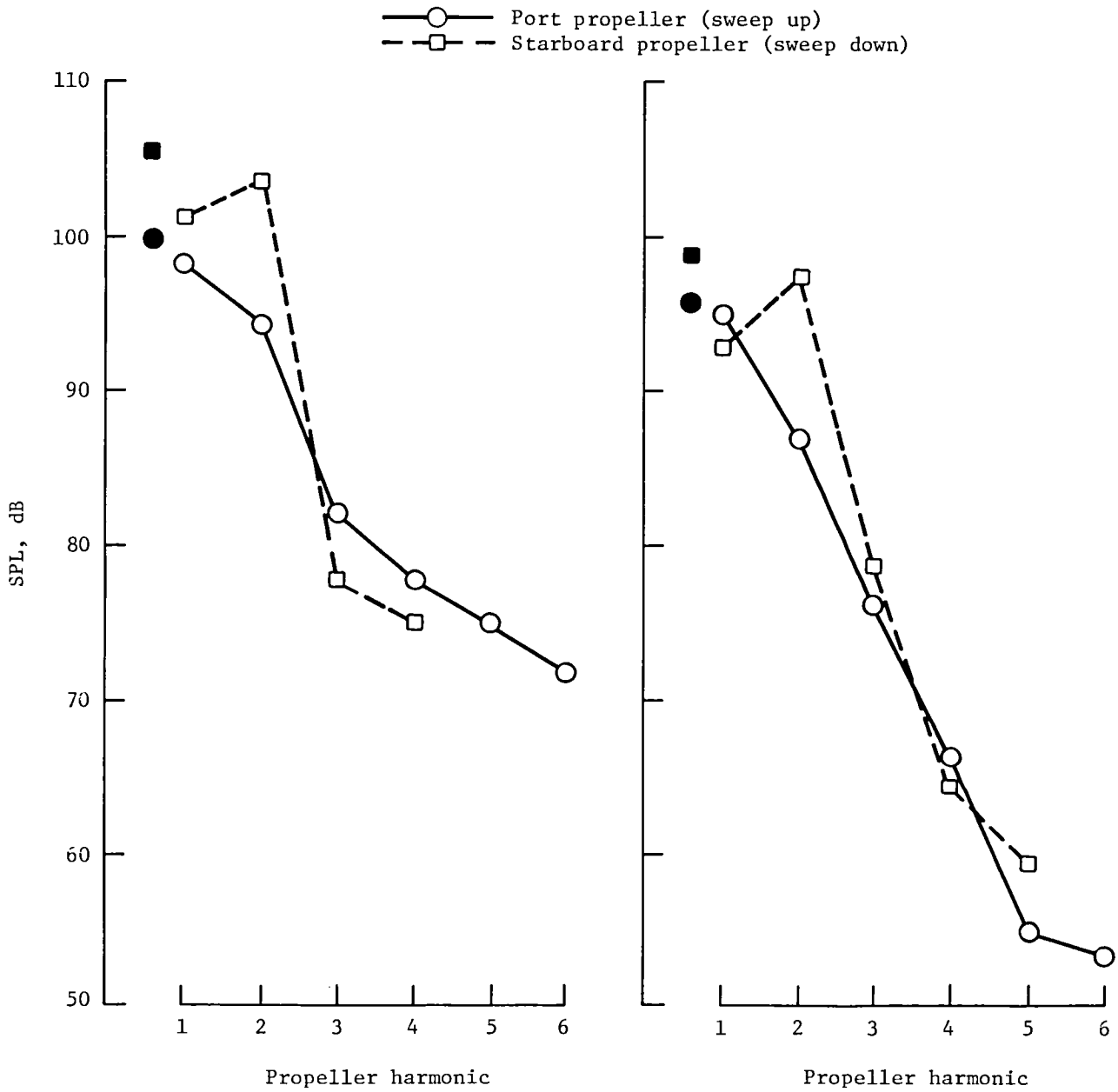

(a) Lined with fiberglass only.

(b) Completely trimmed.

Figure 9. Comparison of interior noise levels due to port and starboard propellers. Four-blade propeller at 1540 rpm; 210-knot airspeed at 3650-m altitude. Solid symbols indicate OASPL.

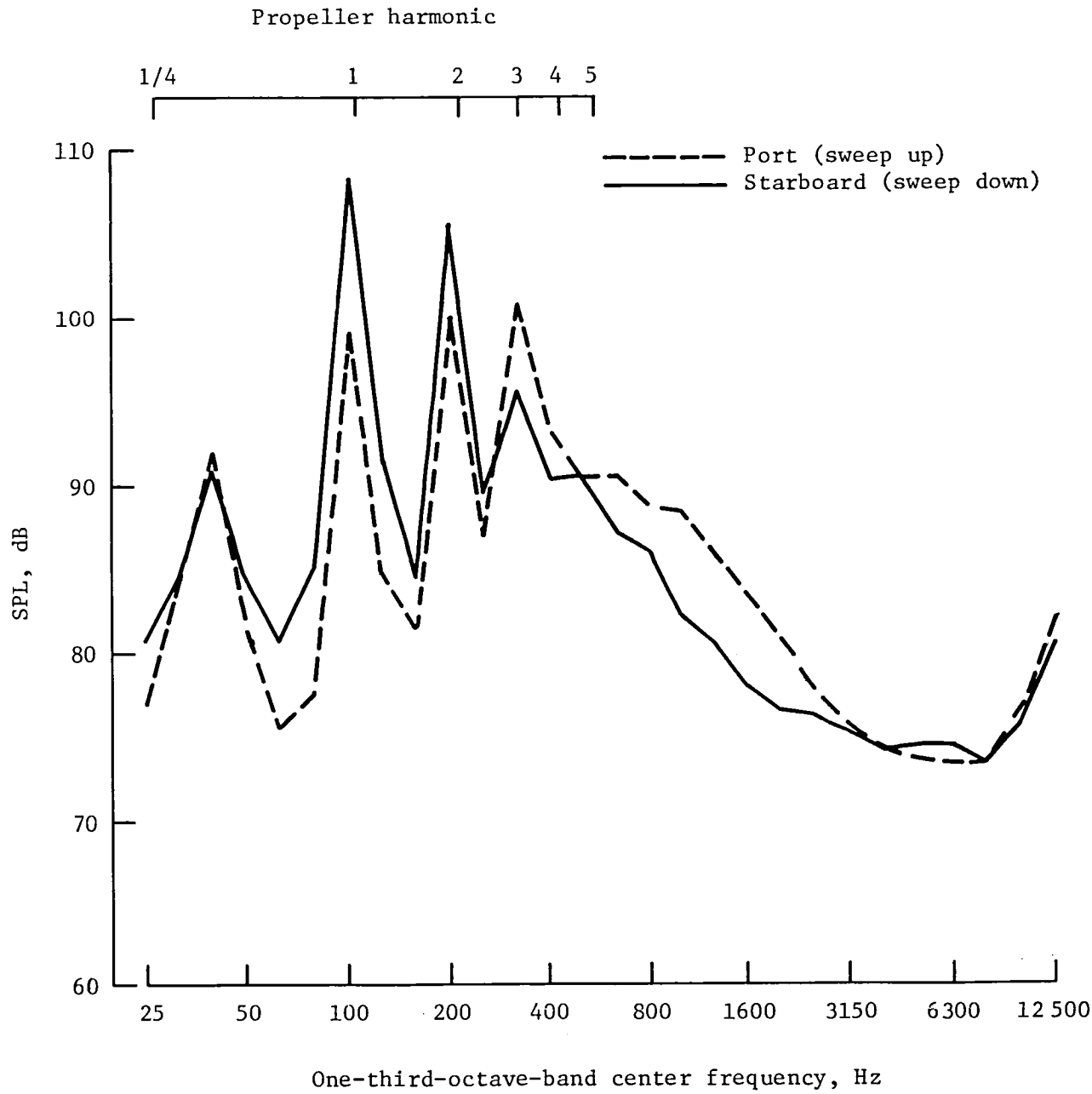

Figure 10. Comparison of averaged interior spectra for ground tests of port and starboard propellers at 1570 rpm on two-engine airplane. $\theta_p = 104°$; ground test of airplane was made before installing trim.

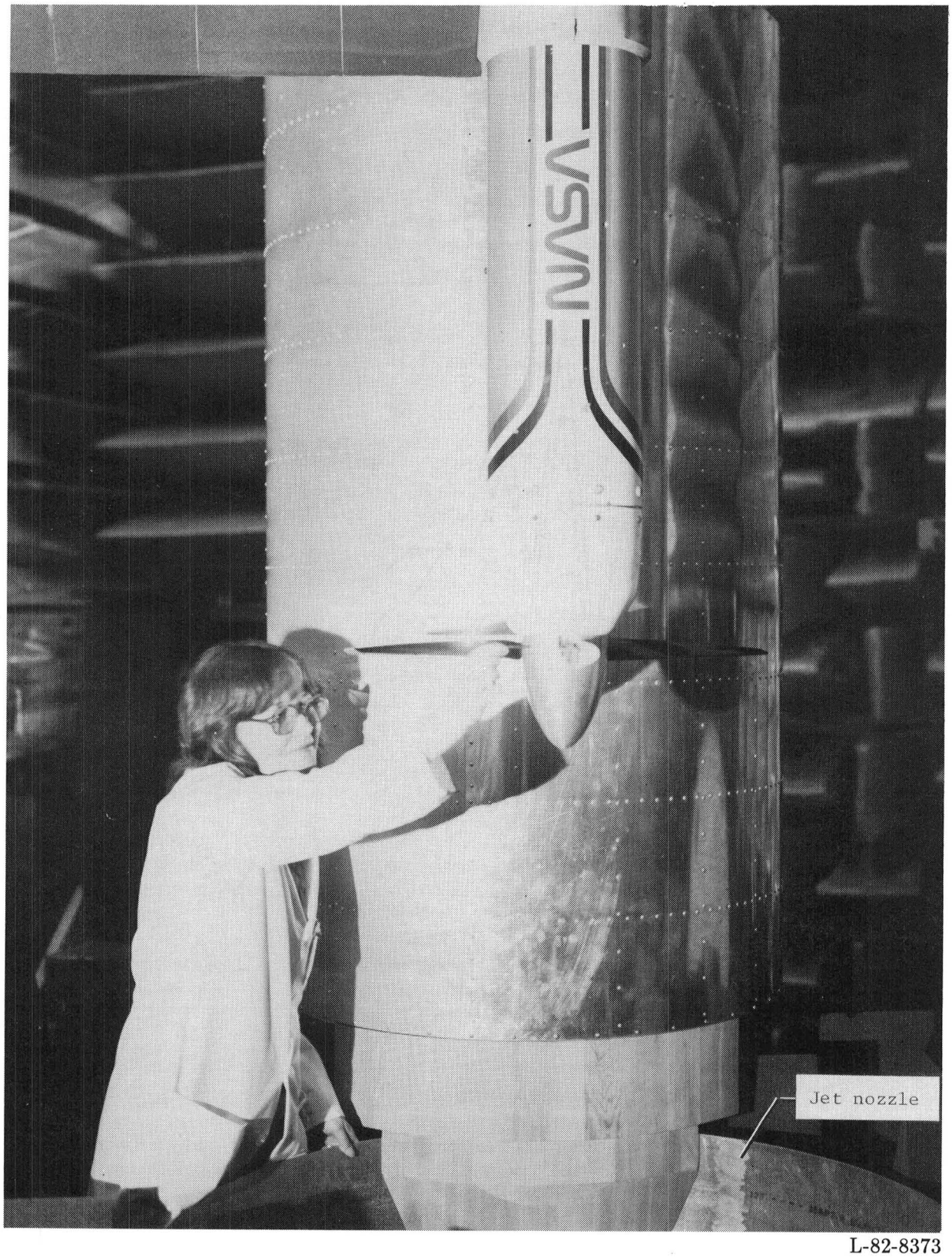

L-82-8373

Figure 11. Photograph of model 2 in the quiet flow facility.

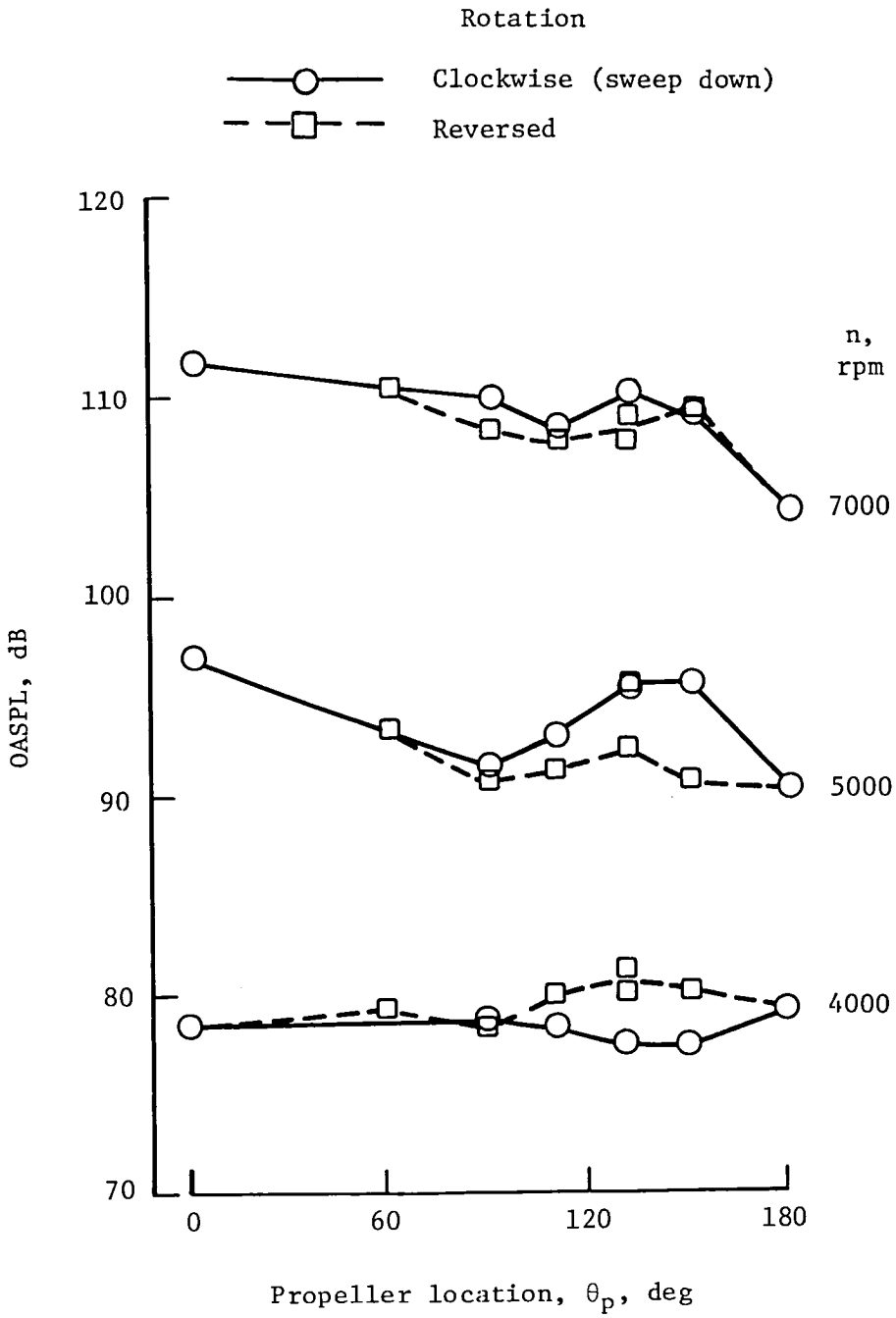

(c) Fuselage lined with damping tape.

Figure 16. Concluded.

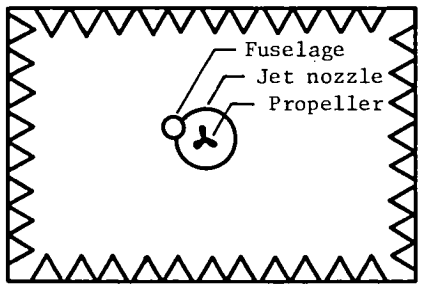

Anechoic room:
Size, 6 × 9 × 12 m;
range, 80 to 30 000 Hz;
absorption coefficient, 0.995

Three-blade propeller,
0.76-m diameter

(a) Plan view of model installation.

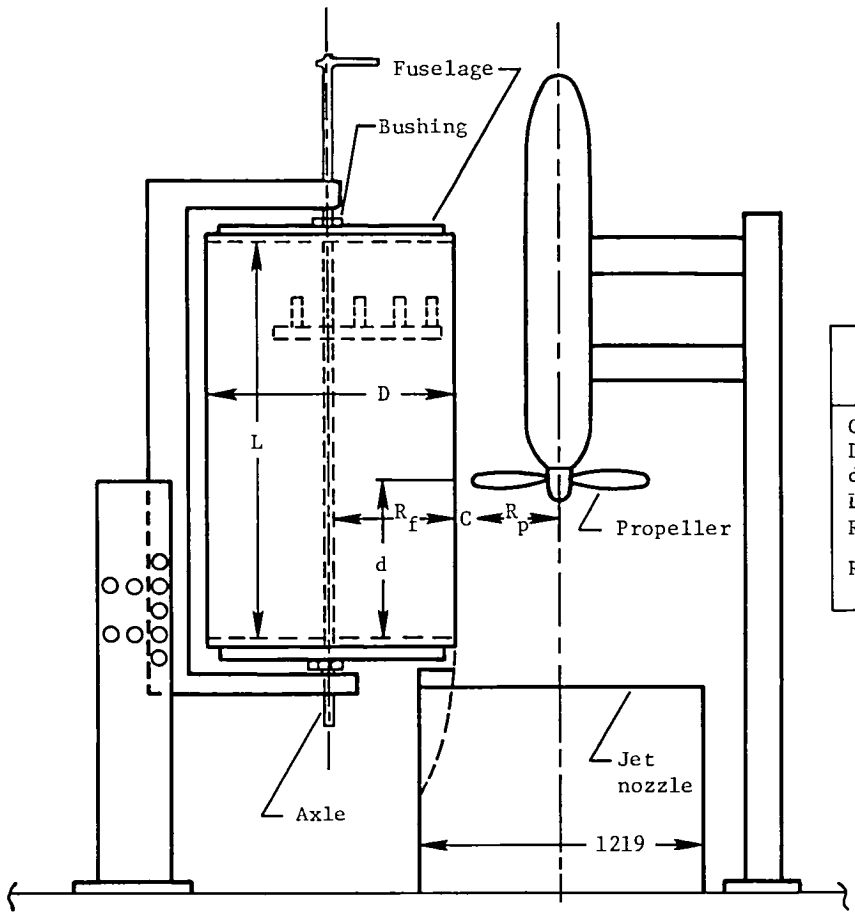

Item	Model		Merlin IVC
	1	2	
C, mm ----	114	76	171
D, mm ----	508	1016	1676
d, mm ----	650	662	
L, mm ----	1194	1803	
R_p, mm ---	381	381	1346
R_p/R_f ----	1.50	0.75	1.61

(b) Model fuselage mounted in anechoic room. Dimensions are given in millimeters.

Figure 12. Schematic diagrams of test facilities and apparatus.

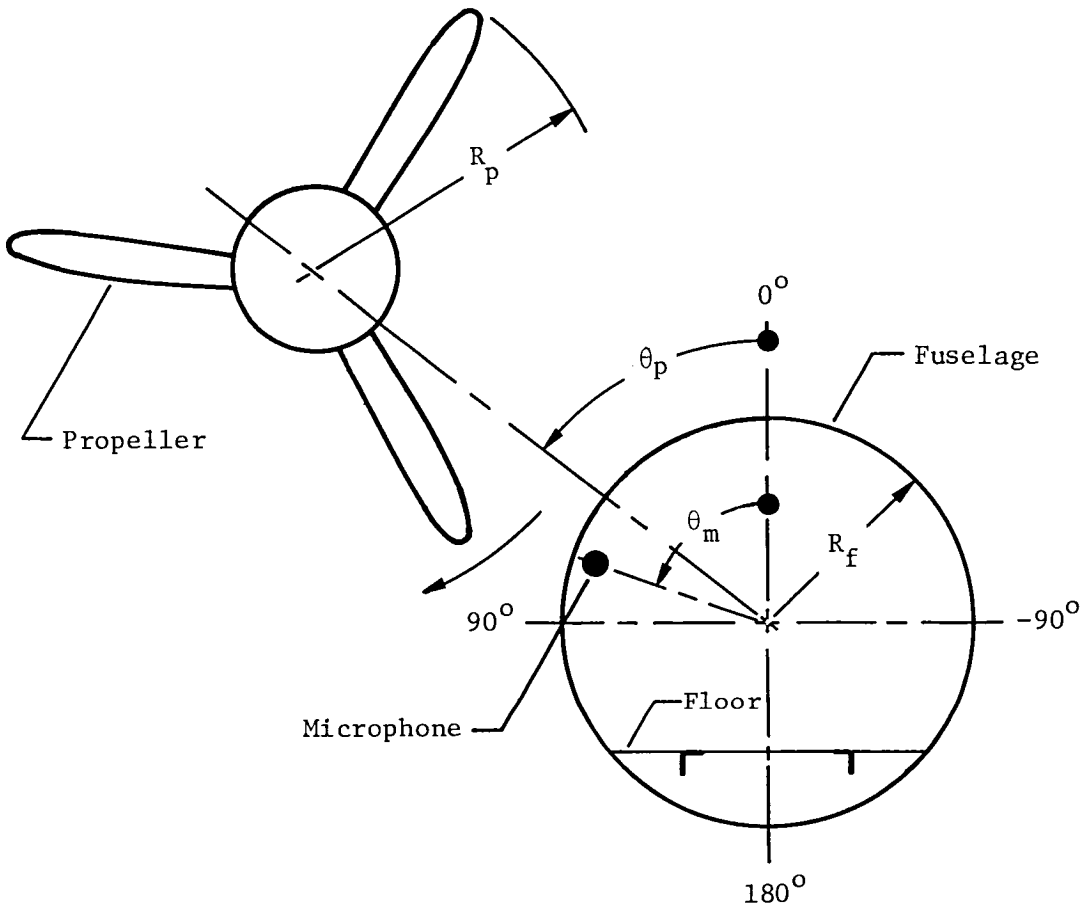

(c) Coordinate system. View looking forward.

Figure 12. Continued.

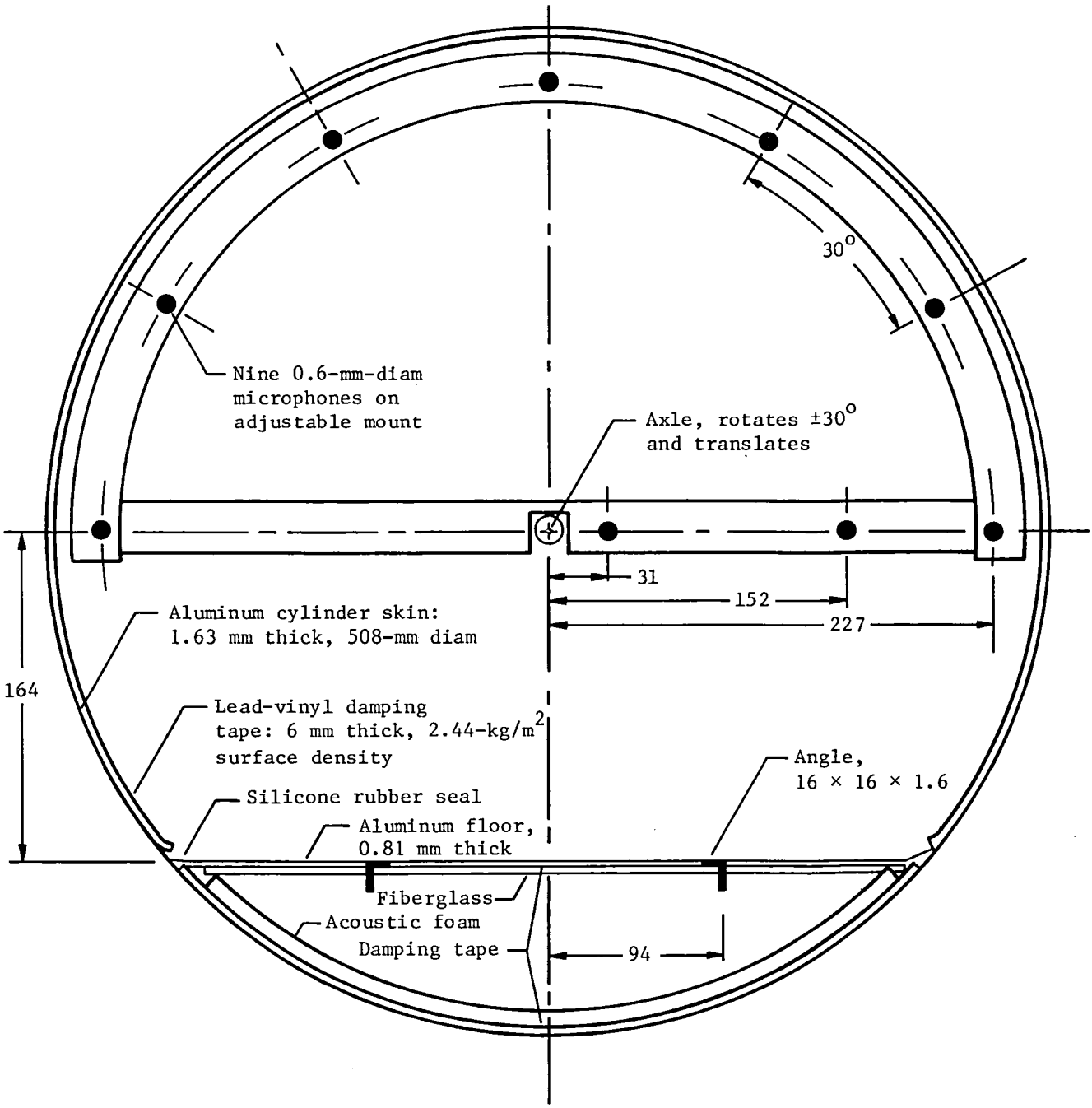

(d) Fuselage details and microphone locations for model 1. Dimensions are given in millimeters unless otherwise specified.

Figure 12. Continued.

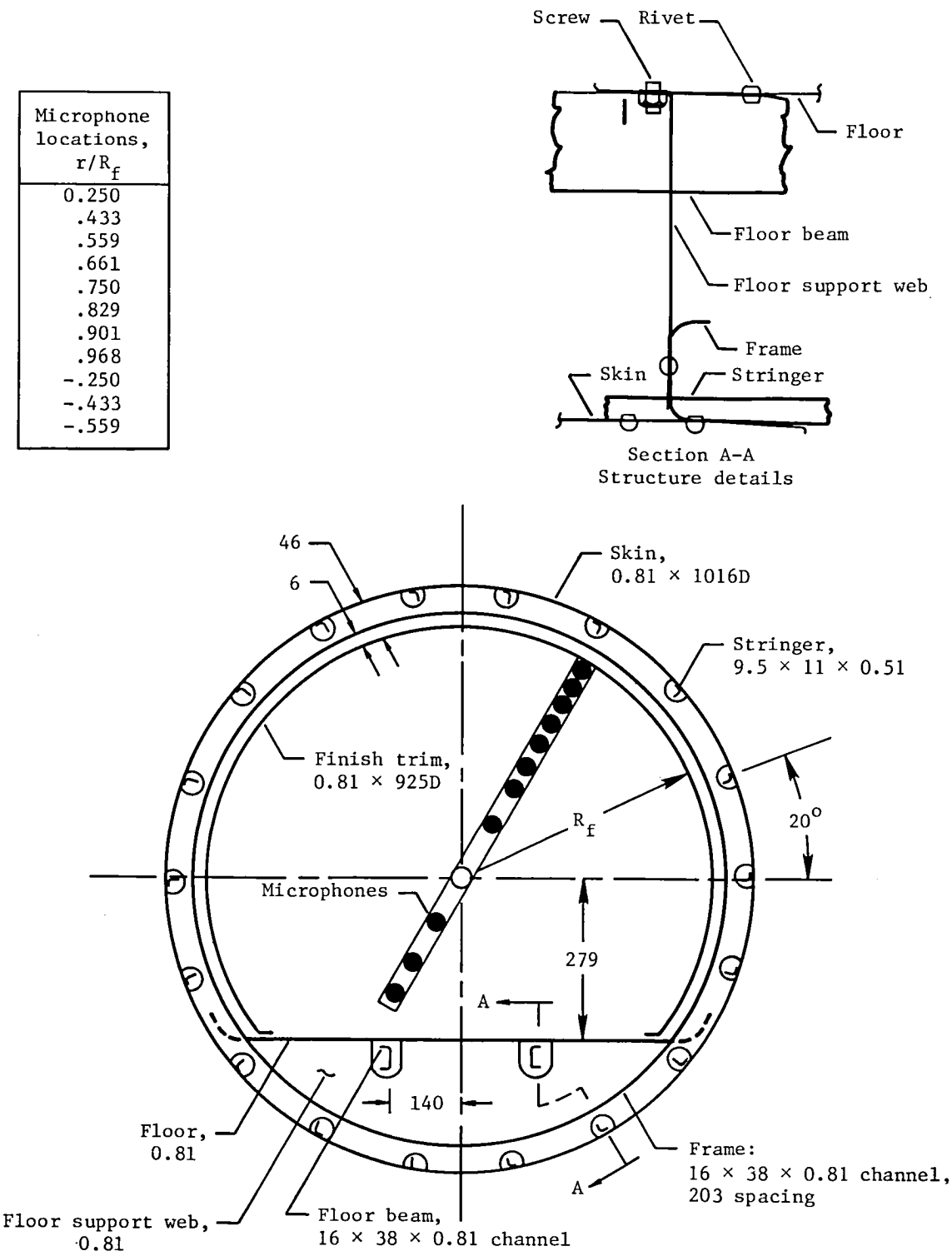

(e) Fuselage details and microphone locations for model 2. Dimensions are given in millimeters unless otherwise specified.

Figure 12. Concluded.

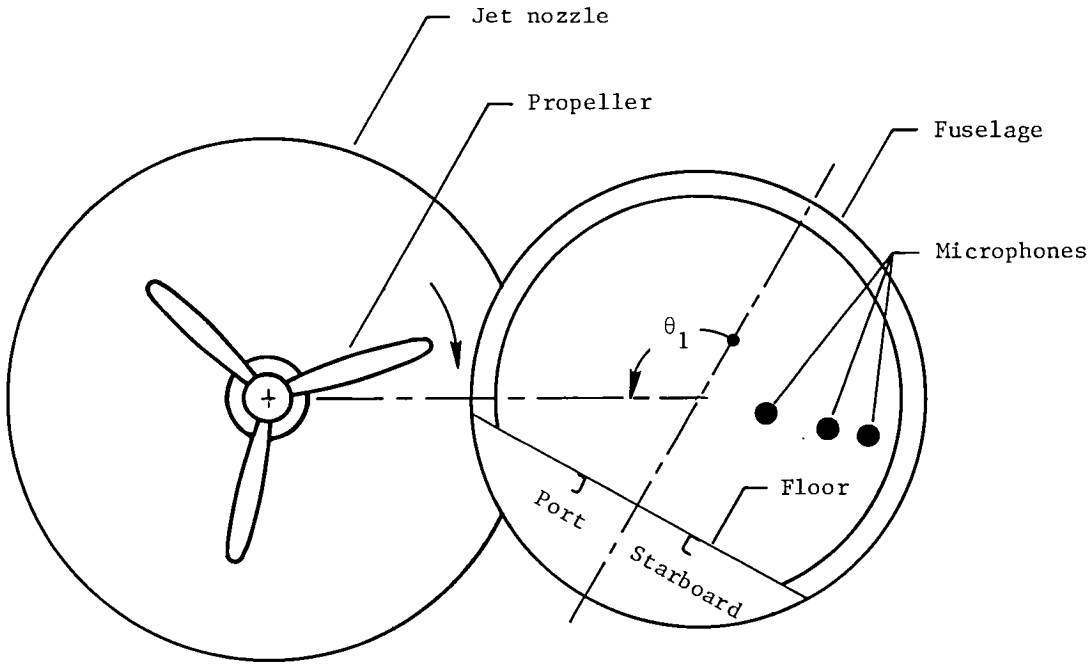

(a) Clockwise rotation; propeller tip sweeps down on port side of fuselage.

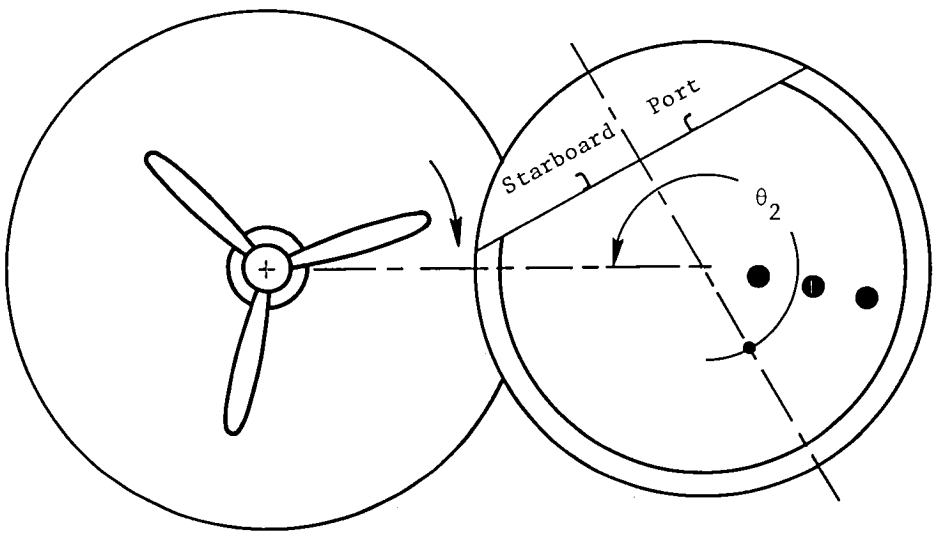

(b) Simulated reversed rotation; propeller tip sweeps up starboard side of fuselage. $\theta_2 = 360° - \theta_1$.

Figure 13. Schematic drawing of test setups for clockwise and simulated reversed rotation of propeller.

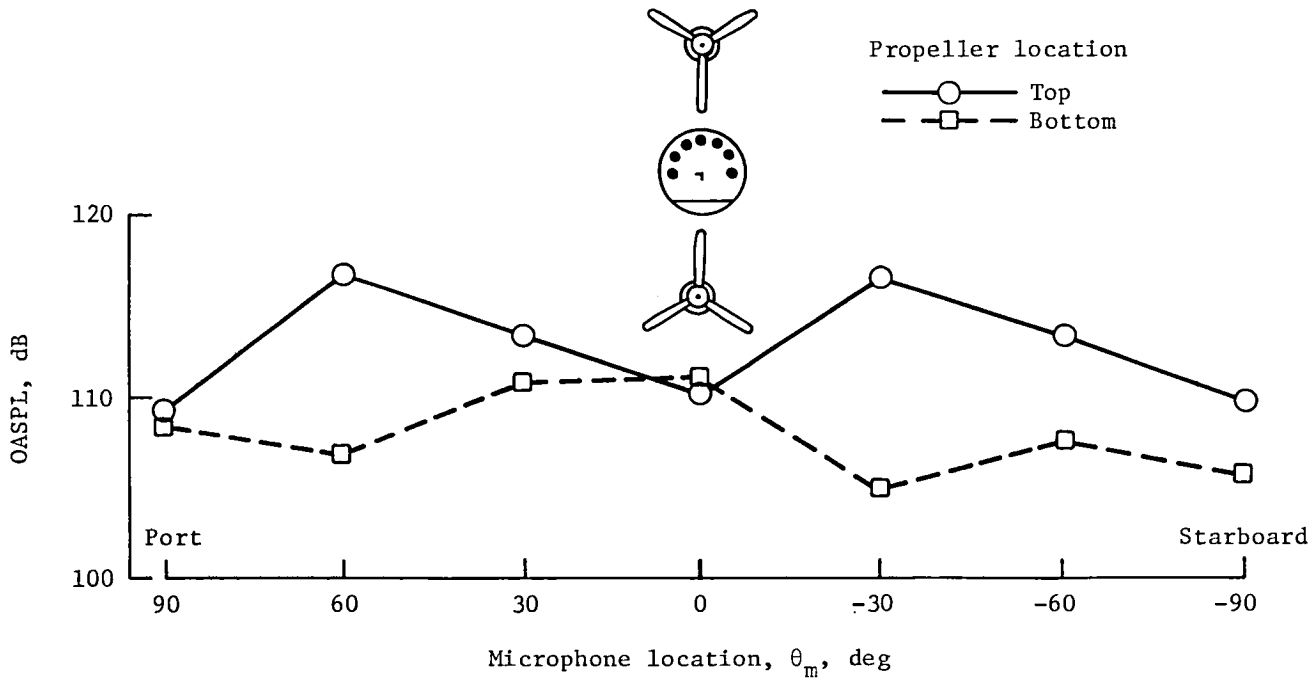

Figure 14. Comparison of interior noise levels for propeller above and below fuselage. Model 1.

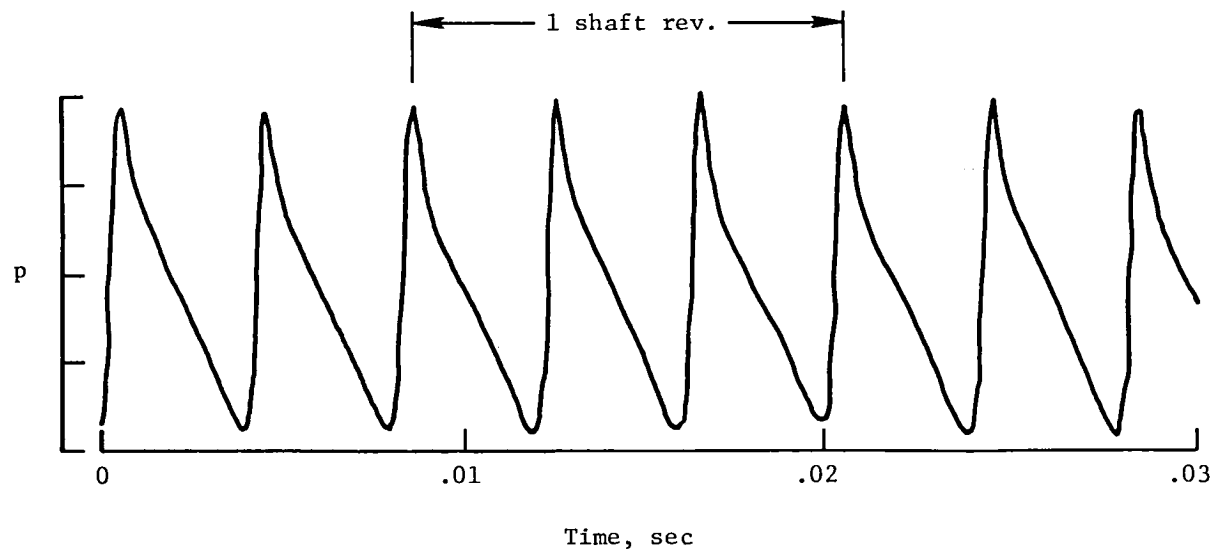

Figure 15. Measured pressure time history of model propeller noise. Propeller plane; $n = 5000$ rpm; free field 8 cm from tip.

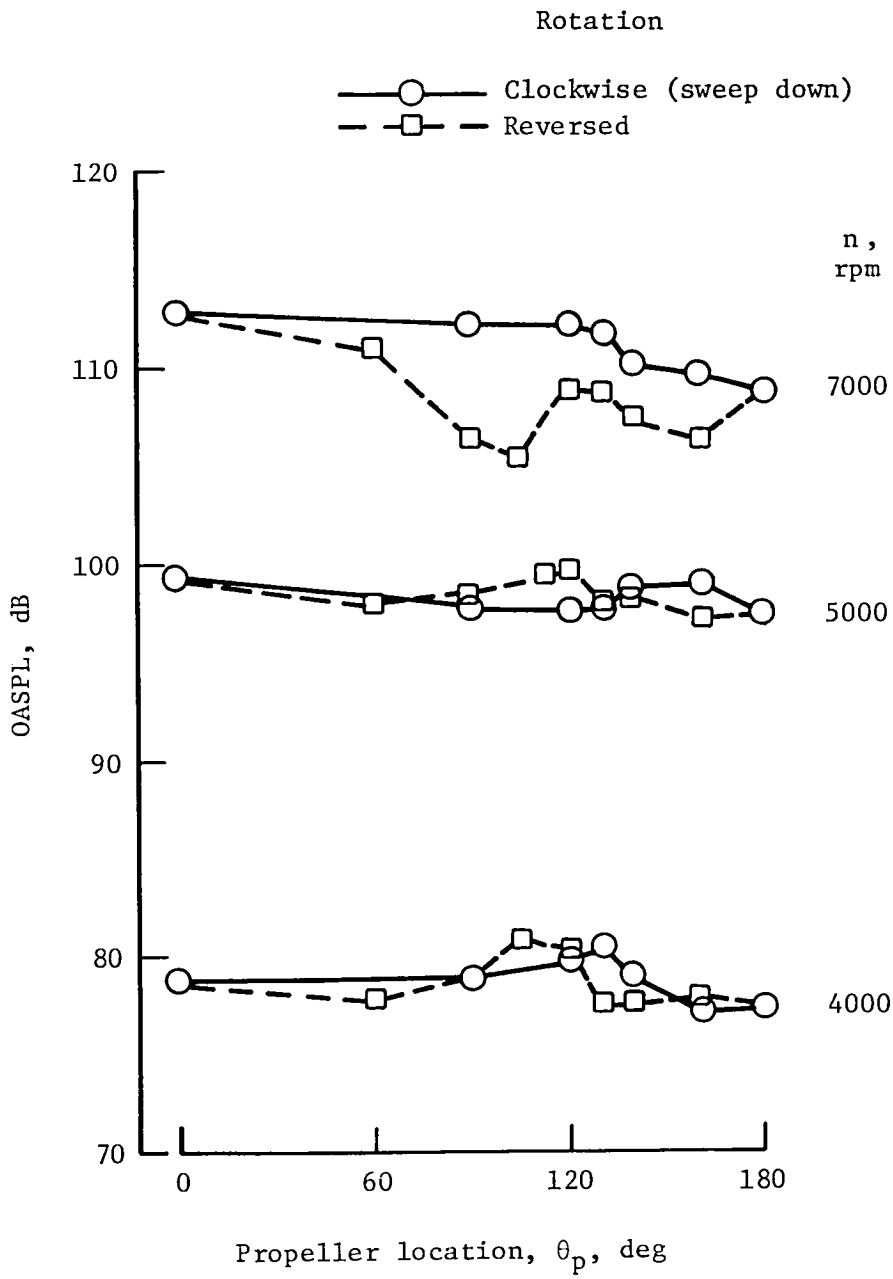

(a) Fuselage lined with 6-mm acoustic foam.

Figure 16. Variation in average interior OASPL with propeller location and direction of rotation for three fuselage trim conditions. Model 1.

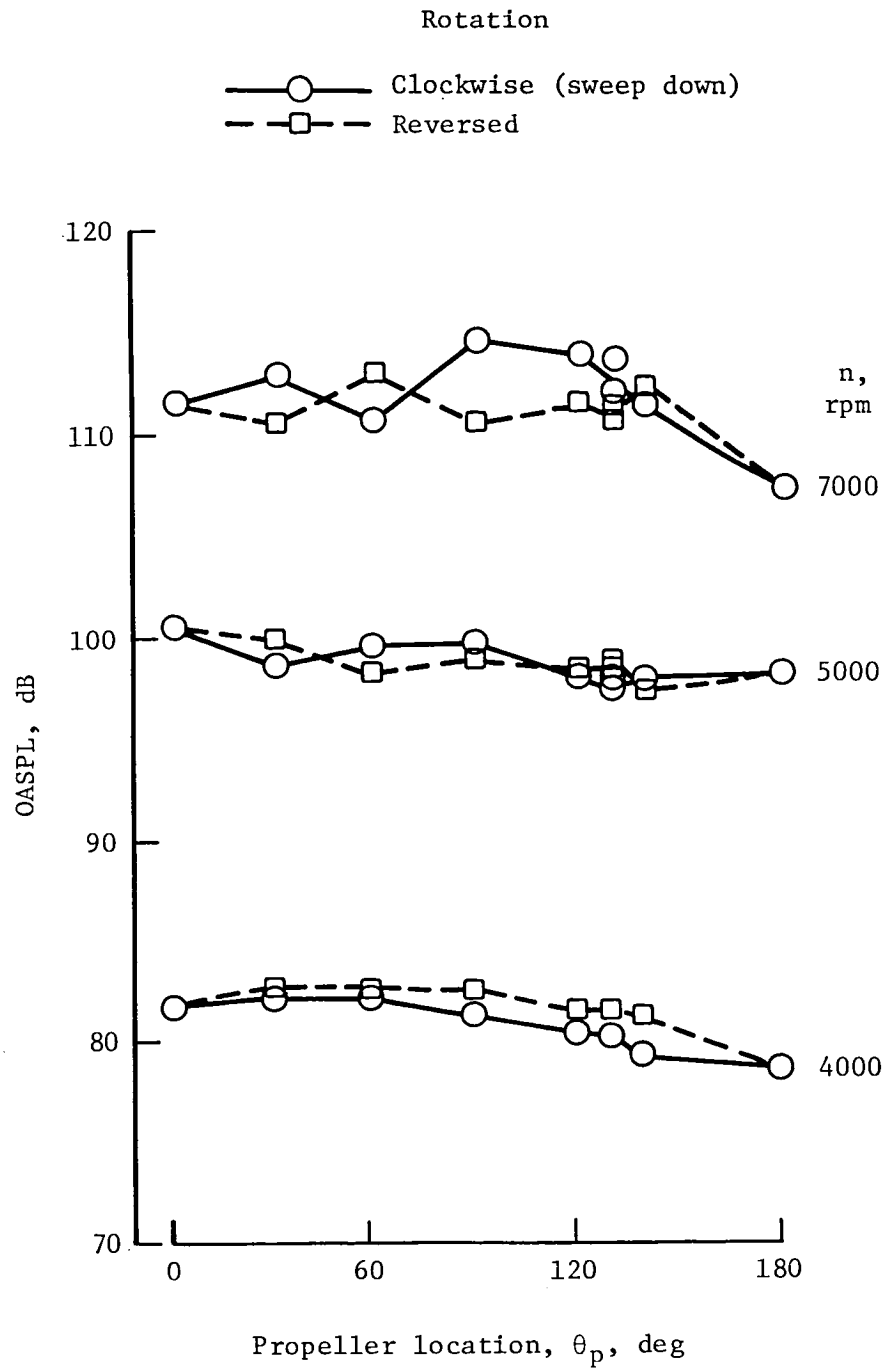

(b) Unlined fuselage.

Figure 16. Continued.

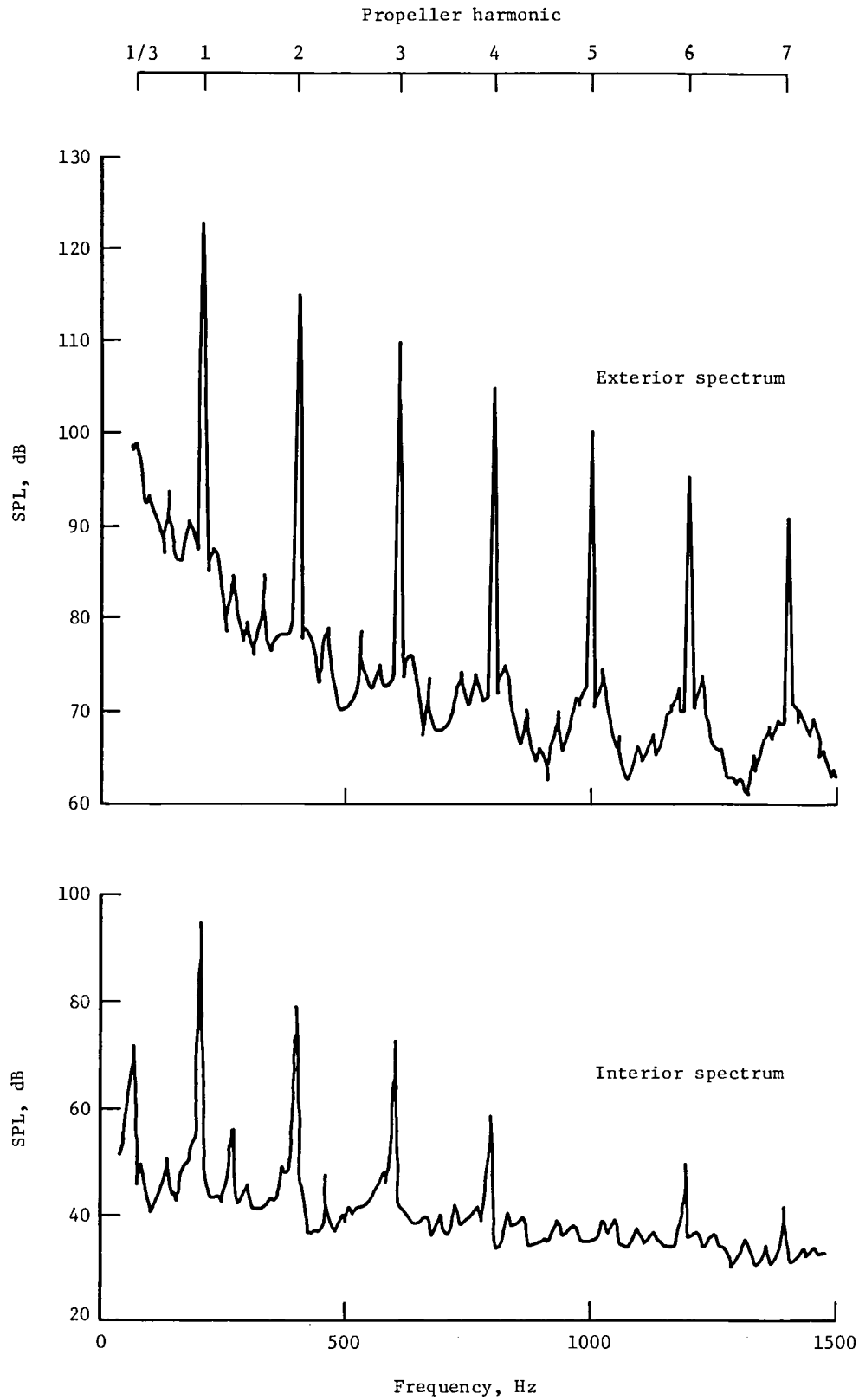

Figure 17. Typical spectrum of exterior noise applied to model and the resulting interior noise. Model 2; $n = 4000$ rpm.

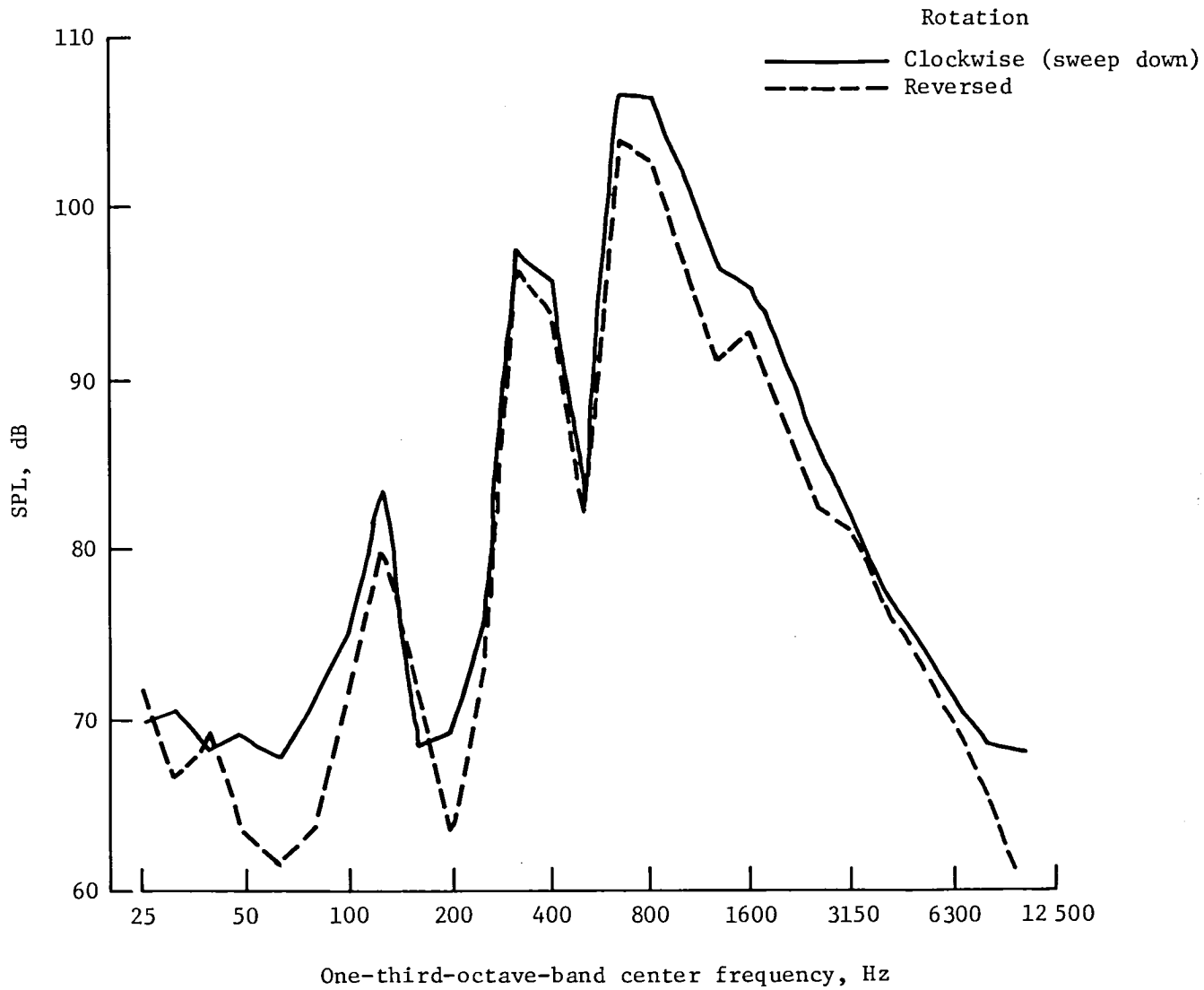

Figure 18. Interior noise spectra for clockwise and reversed rotation of port propeller. Model 1 lined with damping tape; $\theta_p = 130°$; $n = 7000$ rpm.

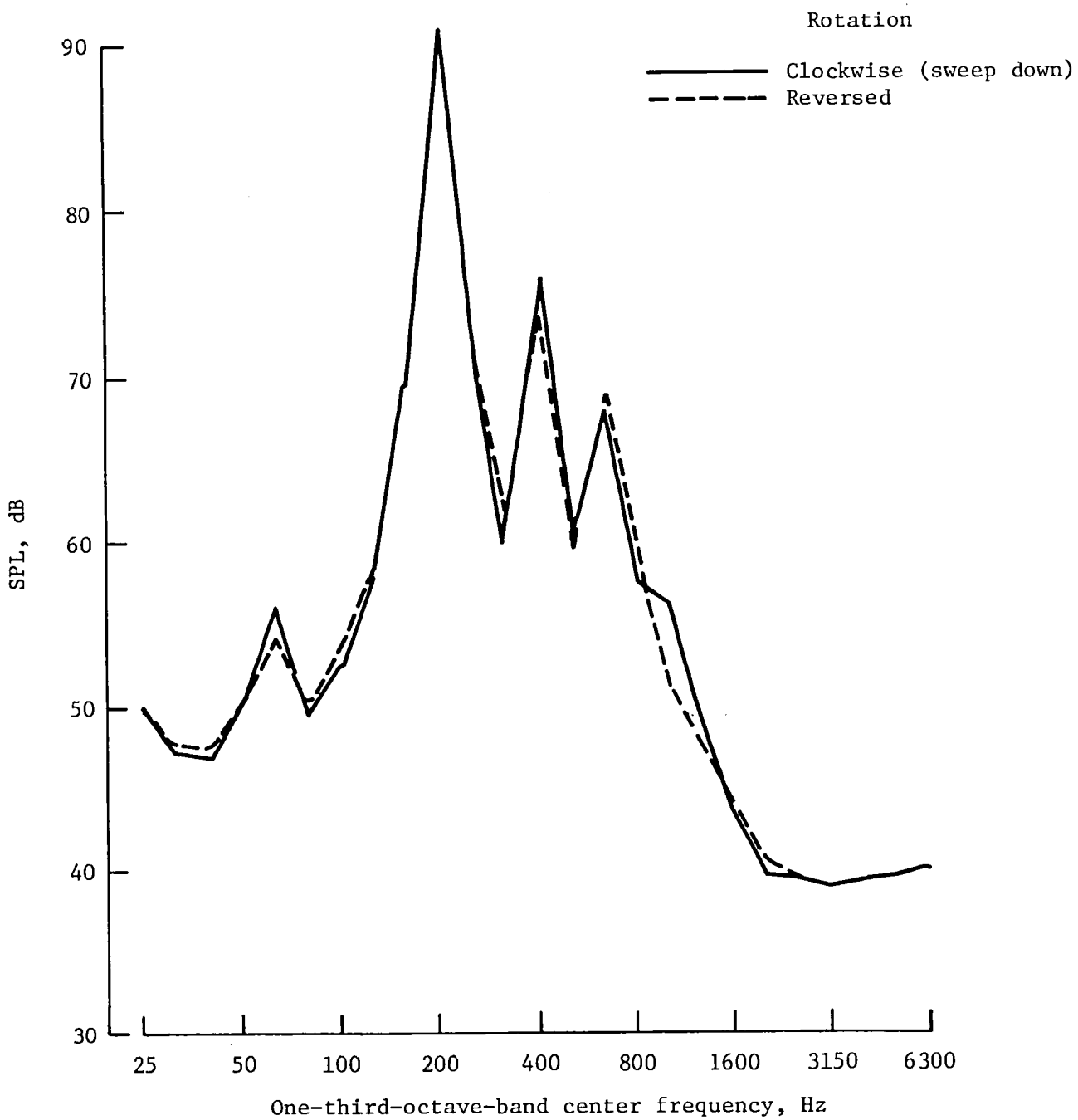

Figure 19. Comparison of space-averaged interior spectra for clockwise and reversed rotation of port propeller. Model 2; $\theta_p = 135°$; $n = 4000$ rpm.

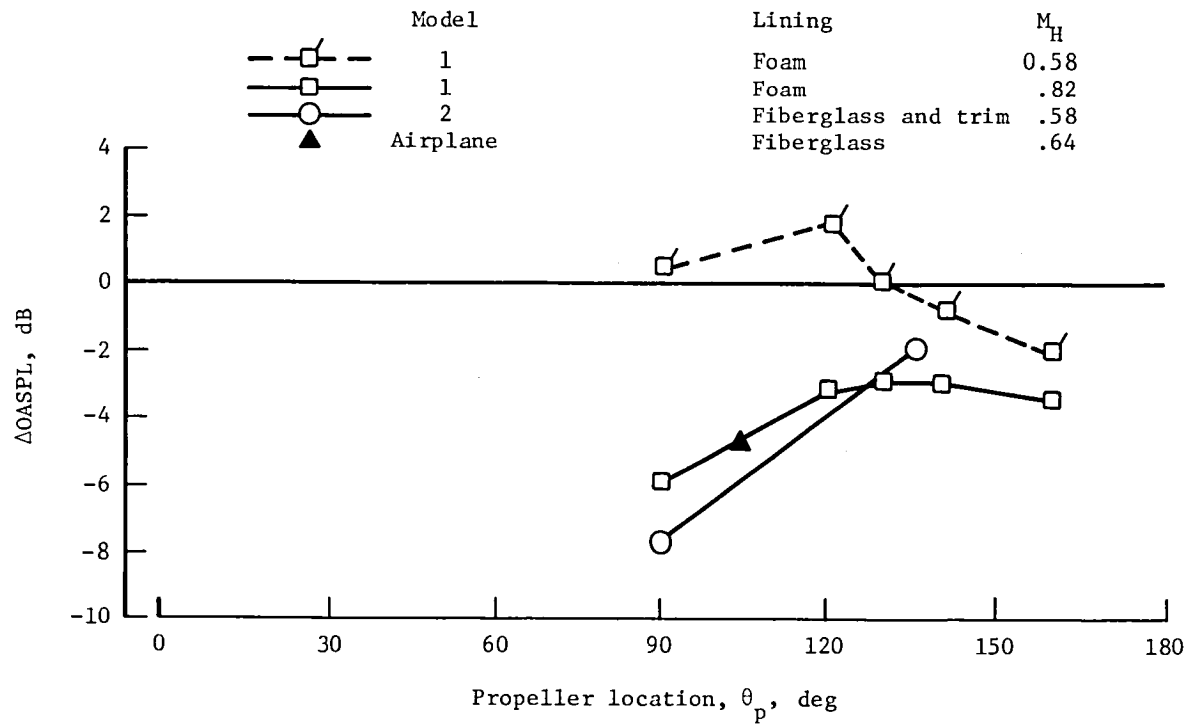

(a) Comparison of three fuselages.

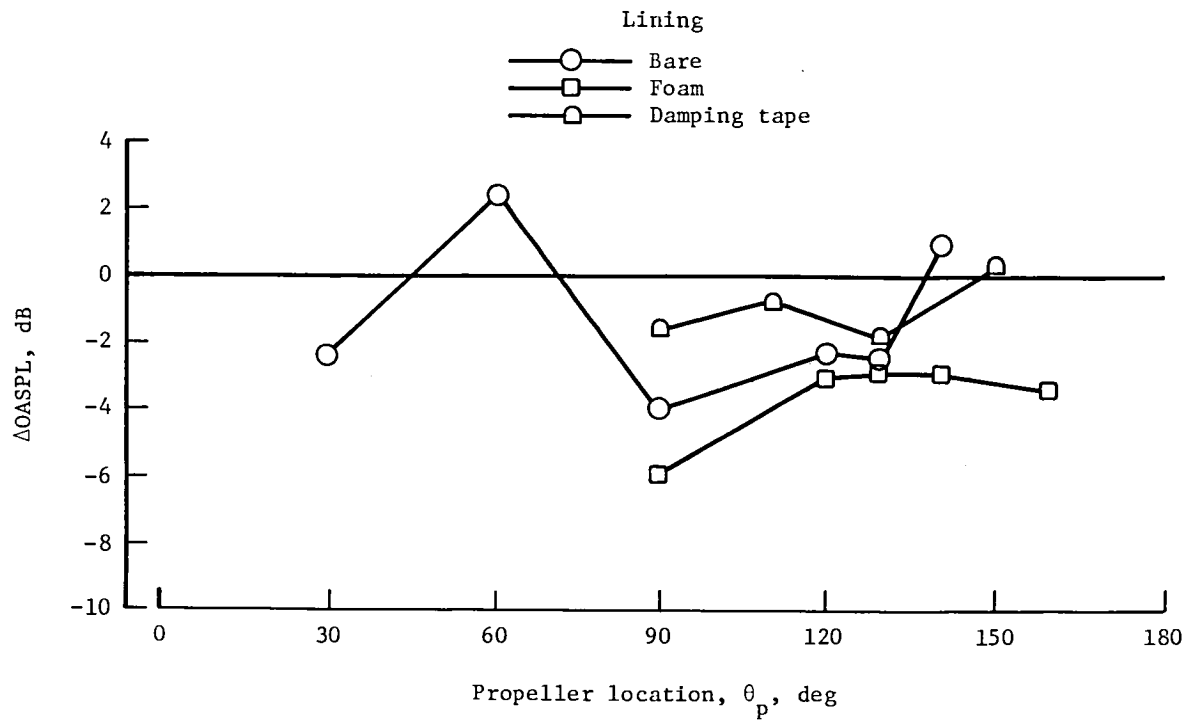

(b) Comparison of three lining conditions. Model 1; $M_H = 0.82$.

Figure 20. Change in average interior noise level ΔOASPL with reversal of downsweeping propeller for various test conditions.

1. Report No.	2. Government Accession No.	3. Recipient's Catalog No.
NASA TP-2444		

4. Title and Subtitle	5. Report Date
Effects of Propeller Rotation Direction on Airplane Interior Noise Levels	July 1985
	6. Performing Organization Code: 505-33-53-03
7. Author(s): Conrad M. Willis, William H. Mayes, and Edward F. Daniels	8. Performing Organization Report No.: L-15892
9. Performing Organization Name and Address: NASA Langley Research Center, Hampton, VA 23665	10. Work Unit No.
	11. Contract or Grant No.
12. Sponsoring Agency Name and Address: National Aeronautics and Space Administration, Washington, DC 20546	13. Type of Report and Period Covered: Technical Paper
	14. Sponsoring Agency Code

15. Supplementary Notes

16. Abstract

Interior noise measurements for upsweeping and downsweeping movement of the propeller blade tips past the fuselage have been made on a twin-engine airplane and on two simplified fuselage models. Changes in interior noise levels of as much as 8 dB for reversal of propeller rotation direction were measured for some configurations and test conditions.

17. Key Words (Suggested by Authors(s))	18. Distribution Statement
Propeller noise Airplane interior noise	Unclassified—Unlimited Subject Category 71

19. Security Classif.(of this report)	20. Security Classif.(of this page)	21. No. of Pages	22. Price
Unclassified	Unclassified	32	A03

For sale by the National Technical Information Service, Springfield, Virginia 22161

NASA-Langley, 1985

National Aeronautics and
Space Administration

Washington, D.C.
20546

Official Business
Penalty for Private Use, $300

BULK RATE
POSTAGE & FEES PAID
NASA Washington, DC
Permit No. G-27

NASA

POSTMASTER: If Undeliverable (Section 158 Postal Manual) Do Not Return